

Upper

N 66-16605

FALLING SPHERE-RADAR MATHEMATICAL SIMULATION TECHNIQUES

FACILITY FORM 602

(ACCESSION NUMBER)	(THRU)
80	1
(PAGES)	(CODE)
CR 170144	13
(NASA CR OR TMX OR AD NUMBER)	(CATEGORY)

by

Forest L. Staffanson
and
Kenneth E. Phillips

Air

GPO PRICE \$ _____

CFSTI PRICE(S) \$ _____

Hard copy (HC) 3.00

Microfiche (MF) 75

FINAL REPORT

Results of Research
Performed Under
NASA Grant
NGR 45-003-016

For the Period

15 December 1964 Through 15 August 1965

Research

ff 653 July 65

Laboratory

University of Utah
Salt Lake City, Utah



FALLING SPHERE-RADAR MATHEMATICAL
SIMULATION TECHNIQUES

FINAL REPORT

(Results of Research Performed Under
NASA Grant NGR 45-003-016

for the period
15 December through 15 August 1965)

by

Forrest L. Staffanson

and

Kenneth E. Phillips

University of Utah
Upper Air Research Laboratory

Obed C. Haycock
Project Director

Obed C. Haycock

Obed C. Haycock

21 Sept. 65

Date

ABSTRACT

16605

In the first part of this report a computer program using Fortran IV is developed which will describe the translational motion of a meteorological sphere falling through the upper atmosphere.

The sphere is assumed a point mass, acted upon by drag, gravity and buoyancy forces. Influence of virtual mass, coriolis and centripetal accelerations are included. The program requires molecular temperature, initial pressure, local mean sea-level gravity and drag coefficients as input quantities.

The output includes position and time data and 24 other variables associated with the sphere flight.

An example illustrating the response of a light sphere to horizontal winds with varying wind layer thickness is presented.

The second part describes a computer program which converts the simulated sphere trajectory into simulated tracking radar data, including radar errors. The results of a preliminary study of an oscillatory error in real ROBIN data is appended.

Autho6

TABLE OF CONTENTS

Part I

Acknowledgments. iii
List of Symbols. v

<u>CHAPTER</u>	<u>PAGE</u>
I. INTRODUCTION	1
II. EQUATIONS OF MOTION.	3
III. EVALUATING EQUATIONS OF MOTION	10
IV. TRAJECTORY GENERATOR PROGRAM	18
V. EXAMPLE.	35
VI. CONCLUSIONS.	42
APPENDIX	43
BIBLIOGRAPHY	50

Part II

Radar Simulator. 51
Appendix, Range Resolver Error 56

LIST OF SYMBOLS

\vec{a}	acceleration of sphere relative to earth-fixed frame.
A	projected cross-sectional area of sphere.
a	semi-major axis of reference earth ellipsoid of revolution.
a_b	acceleration due to buoyancy.
a_c	centripetal acceleration.
a_{c_s}	centripetal acceleration at mean sea level.
a_{cor}	coriolis acceleration.
a_g	gravitational acceleration.
a_{g_s}	gravitational acceleration at mean sea level.
α	ellipticity or flattening of reference ellipsoid.
b	semi-minor axis of reference ellipsoid.
c	speed of sound.
C_d	drag coefficient.
d	sphere diameter.
F_d	drag force.
η	kinematic viscosity.
g	acceleration due to gravity ($ a_g + a_c $).
γ	specific heat ratio of the air.
g'	gravitational acceleration minus acceleration due to buoyancy.
g_s	gravity at mean sea level.
h	geocentric radial component from mean sea level to sphere position.
k	gravitation constant.
L	geocentric latitude.
m	sphere mass without additional apparent mass component.

M	Mach number.
μ	viscosity
M_w	molecular weight of the air.
m_l	total effective mass of the sphere.
ω	earth rotation rate.
ω_c	wind response time constant.
p	sphere position vector.
P	pressure
P_b	pressure at last calculated altitude level.
ϕ	geocentric angular component.
r	geocentric radial component.
R	local geocentric radius of the earth.
R_e	Reynolds number.
R^*	universal gas constant.
ρ	density
T_m	molecular temperature.
\vec{V}	air speed of sphere.
\vec{W}	velocity vector of wind.
z	vertical displacement of sphere.

CHAPTER I
INTRODUCTION

The Langley Research Center of the National Aeronautics and Space Administration has undertaken the responsibility of defining and developing the future operational system for the routine meteorological sounding of the upper atmosphere.

There are presently a variety of methods for obtaining atmospheric measurements, one of which uses a radar-tracked falling sphere. The falling sphere technique is presently used for measuring atmospheric density, temperature and winds. It provides an inexpensive yet reliable method for probing the upper atmosphere.

Under the sponsorship of the above named body, a study was undertaken here at the University of Utah to provide a computerized mathematical simulation program, usable on the IBM 7040 computer. The simulator program was to produce trajectory data of the falling sphere through the upper atmosphere with requirements dictating that this program be versatile, yet provide accuracies as good or better than presently existing falling sphere data processing systems.

Creation of the mathematical simulation program required: (1) development of a mathematical model which could accurately describe the motion of the sphere through the atmosphere, (2) study of available data to determine the computability or tabulation requirements of variables used in the model, and (3) definition of program versatility requirements.

The following pages present the development and results of this study. Because the final objective of this study was to produce a falling sphere simulation program, this report is slanted in this direction by providing not only the development of the mathematical model but a detailed description of the computer program. The limitations of this program as a tool for studying present-existing falling sphere reduction systems, or the development of better future systems, depends in large on the ingenuity of its use.

An example illustrating the program's value and its application to meteorological problems is presented in the closing pages of this report. The results from this example provide information of the sphere's capability in responding to high altitude winds and also indicates areas that may be studied in the future.

CHAPTER II

EQUATIONS OF MOTION

The falling sphere may be represented as a point mass acted upon by gravity, drag and buoyancy forces. Consider the reference frame earth-fixed, with rotation rate ω . The sphere position \vec{p} has a velocity¹ expressed vectorially by

$$\dot{\vec{p}} = \frac{\partial}{\partial t} \vec{p} + \vec{\omega} \times \vec{p} = \vec{v} + \vec{\omega} \times \vec{p} \quad 2-1$$

and acceleration $\ddot{\vec{p}}$;

$$\ddot{\vec{p}} = \vec{a} + 2\vec{\omega} \times \vec{v} + \vec{\omega} \times (\vec{\omega} \times \vec{p}) \quad 2-2$$

where \vec{a} and \vec{v} are respectively the acceleration and velocity of the sphere relative to the earth-fixed frame. The second and third terms of Eq. 1-2 are respectively the coriolis and centripetal accelerations.

The equation of motion is therefore

$$\vec{a} + \vec{a}_c + 2\vec{\omega} \times \vec{v} = \vec{a}_d + \vec{a}_g + \vec{a}_b \quad 2-3$$

where \vec{a}_c = centripetal acceleration

\vec{a}_d = drag acceleration

\vec{a}_b = acceleration due to buoyancy

and

\vec{a}_g = gravitational acceleration.

COORDINATE SYSTEM

The coordinate system chosen is a right-hand orthogonal rectangular coordinate system with its origin located at an arbitrary mean sea level position and whose orientation is such that the z-axis coincides with the geocentric radius vector passing through the coordinate system origin. The y-axis is directed northward and the x-axis eastward.

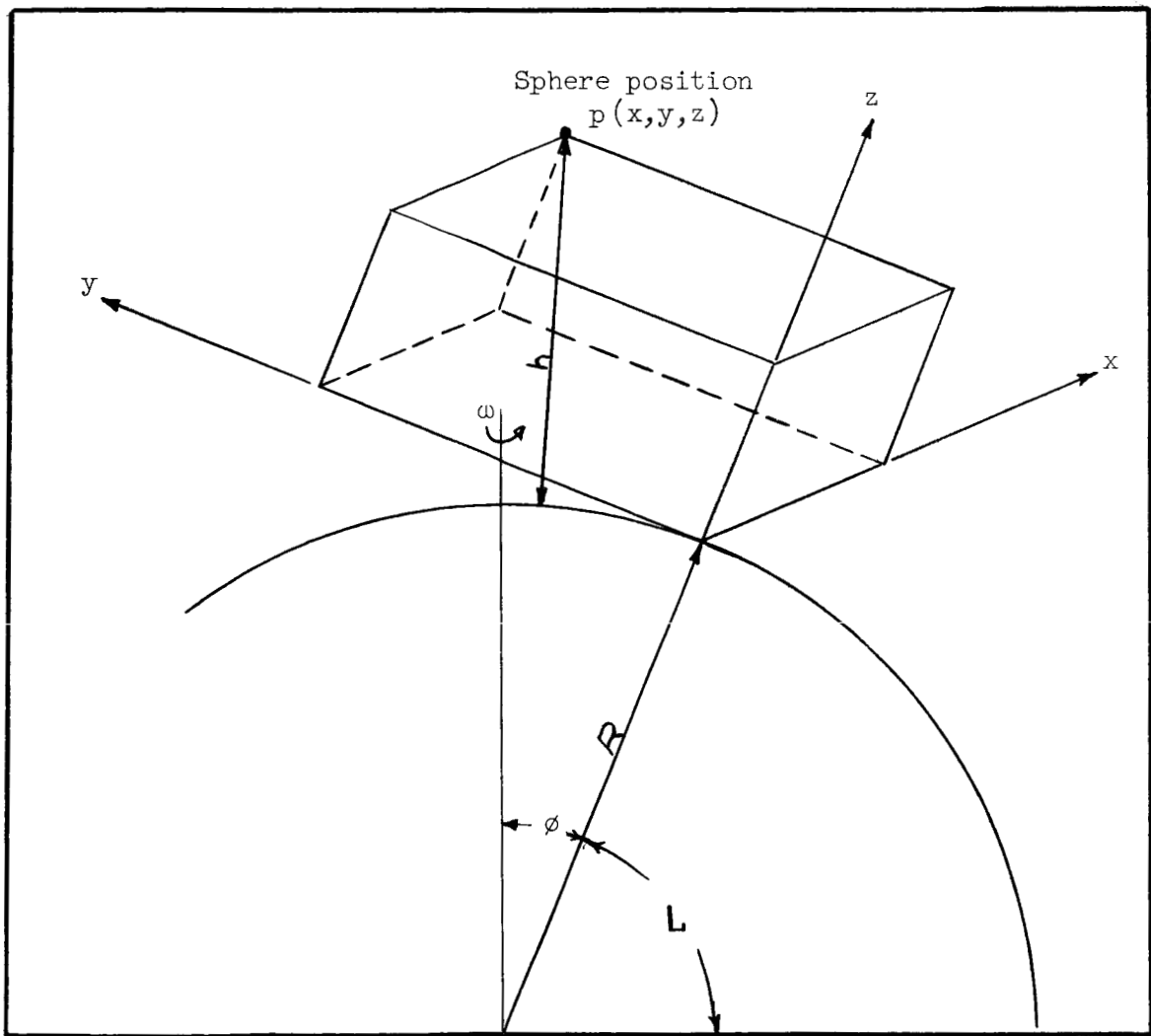


Figure 1: Coordinate System.

CENTRIPETAL ACCELERATIONS

The centripetal acceleration expressed by Eq. 1-4,

$$\vec{a}_c = \vec{\omega} \times (\vec{\omega} \times \vec{p}') \quad 2-4$$

with ω equal to the angular velocity of the earth and \vec{p}' , the positional vector of the sphere, can be expressed using:

$$\vec{\omega} = \omega_1 \hat{y} + \omega_2 \hat{z} \quad 2-5$$

$$\vec{p}' = x \hat{x} + y \hat{y} + (R+z) \hat{z}$$

where $\omega_1 = \omega \cos L$ and $\omega_2 = \omega \sin L$.

Taking the cross product yields:

$$\vec{\omega} \times \vec{p}' = \left[(R+z) \omega_1 \quad -y\omega_2 \right] \hat{x} + x \omega_2 \hat{y} - x\omega_1 \hat{z} \quad 2-5$$

and

$$\begin{aligned} \vec{a}_c = \vec{\omega} \times (\vec{\omega} \times \vec{p}') = & -x \omega^2 \hat{x} + \left[(R+z) \omega_1 \omega_2 - y \omega_2^2 \right] \hat{y} \\ & - \left[(R+z) \omega_1^2 - y \omega_1 \omega_2 \right] \hat{z} \end{aligned} \quad 2-6$$

CORIOLIS ACCELERATION

The coriolis acceleration

$$\vec{a}_{\text{cor}} = 2 \vec{\omega} \times \vec{v} \quad 2-7$$

can be expanded in terms of the rectangular coordinate system. Taking the cross product of the two vectors yields:

$$\vec{a}_{\text{cor}} = (2\omega_1 \dot{z} - 2\omega_2 \dot{y}) \hat{x} + 2\omega_2 \dot{x} \hat{y} - 2\omega_1 \dot{x} \hat{z} \quad 2-8$$

BUOYANCY AND VIRTUAL MASS

The "virtual" or "apparent" mass m_1 is equal to the mass of the sphere plus an additional apparent mass resulting from the momentum transmitted from the sphere to the atmosphere. The ratio of the sphere mass to additional apparent mass is approximately 1/2 for a spherical body.² The effective sphere mass is then

$$m_1 = m + \frac{\pi d^3 \rho}{12} \quad 2-9$$

The buoyancy force is equal in magnitude to the weight of the displaced air and directed opposite to the force of gravity. The effect of buoyancy is introduced by modifying the acceleration \vec{a}_g . By modifying only \vec{a}_g , the slight angular displacement between \vec{a}_g and \vec{g} ,

the acceleration of gravity is neglected. The modified form of \vec{a}_g is given by Eq. 1-10.

$$\vec{g}' = (1 - V_m \rho) \vec{a}_g \quad 2-10$$

where

$$V_m = \frac{\pi d^3}{6m_1}$$

DRAG FORCE

The drag force is given by:

$$\vec{F}_d = -\rho \frac{C_d A}{2} |\vec{V}| \vec{V} \quad 2-11$$

$$\vec{V} = \vec{v} - \vec{W}$$

ρ = air density.

C_d = drag coefficient.

A = sphere cross-sectional area.

\vec{V} = velocity of the body relative to the air.

\vec{v} = velocity of the body relative to the coordinate frame.

\vec{W} = velocity of the air relative to the coordinate frame.

For convenience the quantity ω_c is introduced which is related to the wind response.

$$\omega_c = \frac{C_d A \rho |\vec{V}|}{2m_1} \quad 2-12$$

This is the "corner frequency" of the sphere to fluctuations in the wind encountered in the trajectory.

This is seen from the approximate equation for horizontal speed,

$$\dot{\xi} = -\omega_c (\xi - W_h)$$

which has a "time constant"

$$\tau \dot{\xi} + \xi = W_h \qquad \tau = \frac{1}{\omega_c}$$

The sphere therefore will respond to wind fine structure having layer thickness greater than

$$\lambda = \leftarrow \frac{2\pi V}{\omega_c}$$

The quantity

$$L_W = \frac{V}{\omega_c} = \frac{2m_1}{\rho C_d A}$$

is sometimes called the "characteristic length" associated with the altitude lag of a sphere falling through a constant wind shear. (Reed, W. H., NASA TN D-1821, October 1963).

GRAVITATIONAL ACCELERATION

The gravitational force acts along the geocentric radius and is expressed according to Newton's universal gravitation law. In terms of the rectangular reference frame, the gravitational acceleration at a point p is

$$\vec{a}_g = a_{g_s} \left(\left[\frac{x}{(R+h)} \right] \hat{x} + \left[\frac{y}{(R+h)} \right] \hat{y} + \left[\frac{(R+z)}{(R+h)} \right] \hat{z} \right)$$

2-13

where

a_{g_s} = gravitational acceleration at mean sea level.

R = local geocentric radius.

h = altitude above mean sea level.

The coefficient of \hat{z} , $(R+z)/(R+h)$, will vary from unity by less than 10^{-8} during the sphere flight and will therefore be taken as unity for computational purposes.

EQUATIONS OF MOTION

The results obtained in the previous analysis may be combined to give the following form for the equations of motion used in the trajectory generator program.

$$\ddot{z} = -\omega_c (\dot{z} - W_z) + 2\omega_1 \dot{x} + (R+z)\omega_1^2 - y\omega_1\omega_2 - g'$$

$$\ddot{x} = -\omega_c (\dot{x} - W_x) - 2\omega_1 \dot{z} + 2\omega_2 \dot{y} - g'x/(R+h) + x\omega^2$$

2-14

$$\ddot{y} = -\omega_c (\dot{y} - W_y) - 2\omega_2 \dot{x} - \omega_1 \omega_2 (R+z) + y\omega_2^2 - gy/(R+h)$$

where $\omega_1 = \omega \cos L$ and $\omega_2 = \omega \sin L$.

CHAPTER III

EVALUATING THE EQUATIONS OF MOTION

INTRODUCTION

The equations of motion as given by Eq. 2-14 should adequately describe the sphere motion. Evaluation of these equations require values for: (1) ω_c , which is a function of drag coefficient C_d , cross sectional area of the sphere A , density ρ and air speed $|\vec{V}|$; (2) wind vector, which has x, y, and z, components; (3) gravitational acceleration \vec{a}_g , which is a function of position; and (4) the centripetal and coriolis accelerations. Each of these areas will be discussed individually.

DRAG RESPONSE FACTOR ω_c

As mentioned above, the drag response is basically a function of the drag coefficient C_d , the projected area of the body in the direction of flow A , density ρ and the air speed $|\vec{V}|$.

Drag Coefficient C_d

The coefficient of drag for the sphere problem is normally a function of both Mach number and Reynolds number. These are defined as:

$$M = V/c$$

where V = sphere velocity relative to the wind (air speed), c = local speed of sound and

$$R_e = (V/\eta) d \quad 3-2$$

η = kinematic viscosity, d = sphere diameter.

Speed of Sound

The speed of sound and kinematic viscosity are functions of temperature and density. That is, the speed of sound expressed by the theoretical relationship

$$c = \sqrt{(\gamma R^*/M_w) T_m} \quad 3-3$$

will be considered sufficiently accurate for our purposes.

The specific heat ratio of the air, $\gamma = C_d/C_v$ is taken as exactly 1.40, the molecular weight of the air M_w is taken as 28.9644 (both acceptable to 100 km) and the universal gas constant $R^* = 8314.32$ joules/(°K·kg - mol).

Kinematic Viscosity

The kinematic viscosity η is defined as the ratio of the coefficient of viscosity μ and density ρ . Remaining consistent with the U.S. Standard Atmosphere, 1962 we adopt for the coefficient of viscosity

$$\mu = \frac{1.458 \times 10^{-6} (T)^{3/2}}{T + 110.4} \quad 3-4$$

whose form is derived from kinetic theory and whose constants are empirically adjusted.

Density

Density ρ may be calculated from gravity g and temperature T_m .

Using the hydrostatic and state equations;

$$dP = -\rho g dz \quad 3-5$$

$$\rho = \frac{M_w P}{R^* T_m}$$

pressure P may be obtained as a function of g and T_m . (Molecular temperature T_m must be used since the molecular weight, M_w , is assumed constant). Combining the two equations and separating the variables allows one to obtain P in terms of g and T_m .

$$\frac{dP}{P} = - \frac{M_w g}{R^* T_m} dz \quad 3-6$$

Integrating and taking both sides to the power e , the base of natural logarithms yields

$$\frac{P}{P_b} = \exp \left\{ - \frac{M_w}{R^*} \int_{z_b}^z \frac{g(w)}{T_m(w)} dw \right\}$$

or

$$P = P_b \exp \left\{ - \frac{M_w}{R^*} \int_{z_b}^z \frac{g(w)}{T_m(w)} dw \right\} \quad 3-7$$

Since radar data is desired at 1/10 second intervals, g/T_m is approximately linear between data points. This assumption will be used to obtain P at the (n + 1)st data point. That is:

$$P(n+1) = P(n) \exp \left\{ \frac{-M_w}{2R} \left[\frac{g(n+1)}{T_n(n+1)} + \frac{g(n)}{T_m(n)} \right] \Delta z \right\} \quad 3-8$$

where $\Delta z = z_{m+1} - z_m$.

After obtaining P and then using the equation of state,

$$\rho(n+1) = \frac{M_w P(n+1)}{R * T_m(n+1)} \quad 3-9$$

Temperature

The molecular temperature T_m will be considered as an input quantity. This choice of choosing T_m as an input quantity over ρ is somewhat arbitrary. However, to study sphere phenomena as a function of ρ , a perturbing function $\Delta \rho$ is provided in the program to provide the operator with the option of prescribing ρ directly. However, it is noted that since this perturbation is not reflected in T_m , it must be small.

Drag Tables

When Mach number exceeds 2.5, C_d is considered a function only of Reynolds number. Also, when Reynolds number is less than 50 an extrapolation is used.⁵

$$C_d = 2.5 - .023267 R_e + .00015734 R_e^2 \quad 3-10$$

For the trajectory generator program, the values of C_d will be broken into the major drag tables:

$$(1) C_d (R_e, M) \text{ (table)} \quad 0 < M \leq 2.5 \quad 3-11$$

$$(2) C_d (R_e) \text{ (table)} \quad 2.5 < M \text{ and } 50 \leq R_e \quad 3-12$$

Eq. 3-10 is used when Mach number exceeds 2.5 and Reynolds number is less than 50.

WIND DATA

The wind data for the program must be available as input data. This allows for wind response analysis under widely varying wind conditions. Two requirements seem advisable for wind data: (1) the operator should have the option of using a fine or course wind structure, according to his needs, and (2) the wind structure should be specified in rectangular coordinates to conform with the equations of motion.

GRAVITATIONAL ACCELERATION

The magnitude of the gravitational force on a mass m at mean sea level is given by:

$$a_{g_s} m = \frac{kmM}{R^2}$$

3-13

where

R = local radius of the earth.

k = gravitation constant.

M = mass of the earth.

Likewise, the gravitational force at an altitude h above sea level is

$$a_g^m = \frac{kM}{(R+h)^2} \quad 3-14$$

Thus,

$$a_g = a_{g_s} \frac{R^2}{(R+h)^2} \quad 3-15$$

Eq. 3-15 is a more desirable form for the gravitational acceleration because gravity at mean sea level, g_s , is normally known for the test site at which the simulated flight is to be made,

Expressed vectorially, g_s is given by Eq. 3-16.

$$\vec{g}_s = \vec{a}_{g_s} - \vec{a}_{c_s} \quad 3-16$$

The centripetal component at mean sea level, a_{c_s} , can be calculated using Eq. 2-6 and with the displacement $x = y = z = 0$.

$$a_{c_s} = (R\omega_1\omega_2) \hat{y} - (R\omega_1^2) \hat{z} \quad 3-17$$

Using Eq. 3-16 and 3-17, the magnitude of a_{g_s} in terms of g_s is then

$$a_{g_s} = R\omega_1^2 + \sqrt{g_s^2 - (R\omega_1\omega_2)^2} \quad 3-18$$

or

$$a_{g_s} \doteq R\omega_1^2 + g_s \quad 3-19$$

The geocentric radial component above mean sea level, h , is not directly available for computational purposes. From Figure 1, it is seen that

$$(R+h)^2 = (R+z)^2 + x^2 + y^2 \quad 3-20$$

Expanding Eq. 3-20 and eliminating the R^2 terms yields:

$$h^2 + 2Rh - (2Rz + z^2 + x^2 + y^2) = 0 \quad 3-21$$

Using the first two terms of the binomial series expansion of the quadratic solution of Eq. 3-21 show $h \approx z$. Using this result in Eq. 3-20 gives h as a function of x , y , and z .

$$h = z + (x^2 + y^2)/2R \quad 3-22$$

This varies from h , if the earth were an ideal smooth surface, by less than .025% for $x = y = 100$ km.

The surface of the earth is moderately well represented by an ellipsoid of revolution. Therefore, introducing the geocentric coordinates γ , ϕ , and flattening $\alpha = (a-b)/a$ where a and b are the semi-major and semi-minor axes, respectively, an expression for R can be found.³

$$R = a \left[1 + \left[\frac{1}{(1-\alpha)^2} - 1 \right] \sin^2 \phi \right]^{1/2} \quad 3-23$$

If Eq. 3-23 is expanded in an infinite series expansion and the first three terms are used to approximate R ,

$$R \doteq a \left[1 - (\alpha + \frac{3}{2} \alpha^2) \sin^2 \phi \right] \quad 3-24$$

an error of less than 0.0005% is obtained for $\phi = 45^\circ$.

CENTRIPETAL AND CORIOLIS ACCELERATIONS

The centripetal and coriolis accelerations were derived in Chapter II. For the sphere problem it will be assumed that the deviation from latitude L during the flight will be negligible. This is in keeping with the other assumptions if x and y are less than 100 km.

CHAPTER IV

TRAJECTORY GENERATOR PROGRAM

Fortran IV was used to program the equations discussed in Chapters II and III. The computer program consists of a main program and four subroutines used for evaluating the equations of motion. To assist the user of the program in simulating sphere flights under widely varying conditions, this section contains an alphabetical listing and a brief explanation of variables calculated or brought into the MAIN program. A listing of the total program with a flow diagram is contained in the Appendix.

The method selected for explaining the program listing is a line-by-line description of each part of the program with the line numbering system starting anew with each subroutine program.

CODING

Introduction

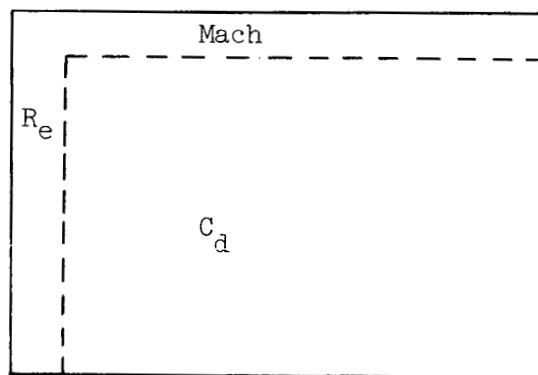
The variables used in the Main Program are listed alphabetically below with a brief explanation of each.

Listing

The variables and arrays are:

A(4)	Array of coefficients used in the Runge-Kutta-Gill integration program.
A21 A22	Constants used in determining data at specified interval levels.
AC	Absolute magnitude of the sphere acceleration relative to fixed frame.
ALPHA	Coefficient associated with the induced virtual mass of the sphere. It should equal 0.5 for inclusion or 0.0 for excluding the induced mass.

ALPHA2	The shape of the earth is moderately well represented by an ellipsoid of revolution. ALPHA2 is the flattening of this reference ellipse.
B(4)	Coefficient array used in Runga-Kutta-Gill integration method.
BET	Buoyancy coefficient. (It should equal 1.0 to include or 0.0 to exclude buoyancy force.)
BETA (2,8)	Coefficients used in Adams-Moulton ⁶ integration method.
C(4)	Coefficient array used in Runga-Kutta-Gill integration method.
CD	Drag Coefficient.
CDREM (22,18)	Array of drag coefficients which are a function of both Reynolds and Mach Numbers. (The array must be read in columnwise and such that Reynolds and Mach numbers are included in the array.)



Tabulated Form

D	Sphere diameter
DELROE	Density perturbation.
DER(1)	\dot{z} , vertical component of sphere velocity,
DER(2)	\dot{x} , Easterly component of sphere velocity.

DER(3)	\dot{y} , Northerly component of sphere velocity.
DER(4)	\ddot{z} , vertical component of sphere acceleration.
DER(5)	\ddot{x} , Easterly component of sphere acceleration.
DER(6)	\ddot{y} , Northerly component of sphere acceleration.
F(1)	t, time in seconds.
F(2)	z, sphere altitude in meters.
F(3)	x, displacement of sphere in the Easterly direction.
F(4)	y, displacement of sphere in the Northerly direction.
F(5)	\dot{z} , vertical velocity of sphere.
F(6)	\dot{x} , Easterly component of sphere velocity.
F(7)	\dot{y} , Northerly component of sphere velocity.
F(8)	W_z , Easterly component of wind velocity.
F(9)	W_x , Westerly component of wind velocity.
F(10)	W_y , Westerly component of wind velocity.
F(11)	V, magnitude of sphere velocity relative to the wind.
F(12)	a, magnitude of sphere acceleration relative to earth fixed frame.
F(13)	$\Delta\rho$, density perturbation.
F(14)	\ddot{z} , vertical component of sphere acceleration.
F(15)	\ddot{x} , Easterly component of sphere acceleration.
F(16)	\ddot{y} , Northerly component of sphere acceleration.
F(17)	\ddot{z}_d , vertical component of drag acceleration.
F(18)	\ddot{x}_d , Easterly component of drag acceleration.
F(19)	\ddot{y}_d , Northerly component of drag acceleration.
F(20)	ρ , density.
F(21)	T_m , molecular temperature.

F(22)	M, Mach number.
F(23)	R_e , Reynolds number.
F(24)	C_d , Drag coefficient.
F(25)	P_b , Pressure at altitude z.
F(26)	V_t , Terminal velocity.
F(27)	g, Gravity.
FT(J)	The array FT(J) is equivalent to the array F(J) at time (t-h) seconds.
FNC(6,8)	Array of integrated values of the derivative equations DER(6) for the past NM time values. (Note: NM should not be larger than 8 unless the corresponding Dimension Statements are changed.)
F2	Altitude z at time (t-2h) seconds.
GAMMA (2,8)	Coefficients associated with Adams-Moulton integration method.
GS	g_s , the value of g at mean sea level for test site.
H	h, time interval used in integration program.
IT	Row index of the data table ZTZXY.
JT	Column index for ZTZXY data table.
KOLD	If during the flight, any one of the variables M, R_e , or z exceed the bounds prescribed by the input tables, the constant KOLD is set equal to unity, causing a diagnostic to be printed and the flight to be stopped.
KI	Row index in drag table.
KO	Row index in data table ZTZXY.
L1	Total number of rows in data table ZTZXY.
L2	Total number of rows in drag table CDREM.
L3	Total number of columns in drag table CDREM.
L4	Total number of rows in drag table RECD.

L21	Variables used in determining data at altitude intervals of ZINT.	
L22		
LA1	Number of steps performed using the single-step integration subroutine.	
N	Number of differential equations.	
NM	Order of polynomial used in multistep integration method.	
NØ	Integer used to eliminate computation of pressure P_b on first cycle.	
NOTAPE	Option indicator for writing data tape. If it is set equal to 1, no tape will be written for the flight. If NOTAPE does not equal 1, a tape will be written.	
Ø1	$2\omega\cos L$	
Ø2	$2\omega\sin L$	
Ø3	$\omega^2 \sin L \cdot \cos L$	
Ø4	$\omega^2 \cos^2 L$	(Flight constants where ω = earth rotational rate, L = latitude.)
Ø5	$\omega^2 \sin^2 L$	
Ø32	$2\omega^2 \cos^2 L$	
ØC	$\frac{\pi d^2 C_d V}{8 m_1}$	
ØC1	$\frac{\pi}{8} d^2$	
ØM	ω^2	
PB	P_b , Pressure.	
Q(6)	Array used in Runge-Kutta-Gill integration method.	
Q1	$\frac{M_w}{R^*}$, Ratio of molecular weight to gas constant.	
QM	M, Mach number.	
QLAT	L, Geocentric latitude in radians.	
R	Geocentric radius for latitude L.	

RL	$1/(2R)$
RADA	Radius of semi-major axis of ellipsoid of revolution which approximates shape of the earth.
RE	R_e , Reynolds number.
RECD(24,2)	Drag table which is a function only of Reynolds number.
RØE	ρ , Density.
SM	m, Sphere mass in kilograms.
SUM(6)	Array used in multi-step integration method.
T	T_m , Molecular temperature.
TI	t, Time in seconds.
TO	Maximum time in seconds allowed for flight.
V(1)	Sphere altitude.
V(2)	T_m
V(3)	W_z (A linear interpolation is used to obtain these values from array ZTZXY.)
V(4)	W_x
V(5)	W_y
V(6)	g, Acceleration due to gravity.
V5	V_t , Terminal velocity.
VEL	V, Velocity of the sphere relative to the wind velocity.
VØL	Sphere volume.
XD2	x_d , x-component of drag acceleration.
Y(1)	z, Sphere altitude in meters.
Y(2)	x, Displacement of sphere in the Easterly direction.
Y(3)	y, Displacement of sphere in the Northerly direction.

Y(4)	\dot{z} , Vertical velocity of the sphere.
Y(5)	\dot{x} , Easterly component of sphere velocity.
Y(6)	\dot{y} , Northerly component of sphere velocity.
YD2	\ddot{y}_d , Component of drag acceleration in Northerly direction.
ZINT	Altitude interval at which data is desired.
ZD2	\ddot{z}_d , Vertical component of drag acceleration.
Z01	Minimum altitude allowed for the flight.
ZTZXY(L1,5)	Data array having: (1) altitude z in 1st column, (2) molecular temperature T_m in second column, (3) z component, x component, and y components of wind velocity in columns 3 through 5, respectively.

MAIN PROGRAM

Introduction

The main program is used principally for inputting and outputting data. It is also used, however, to obtain data at desired interval levels of altitude z , and to perturb ρ , if the user so desires.

Description

- Lines 1-7 Contain the dimension statements of the MAIN program and the common statements used throughout the simulator program.
- Line 8 Statement no. 1. This format statement is used for reading in the parameters more directly associated with the flight as: (1) inclusion or exclusion of induced virtual mass or buoyancy force, (2) time increment used for numerical integration purposes, (3) size of data arrays, (4) polynomial order used in integration method and, (5) option of not printing data flight tape.

<u>Column</u>	<u>Format</u>	<u>Variable</u>	<u>Description</u>
1-5	xx.xx	ALPHA	Coefficient for including or excluding induced virtual mass. For inclusion, it will equal 0.5.
6-10	xx.xx	BET	Coefficient for excluding buoyancy force. It normally will equal 1.0.
11-15	xx.xx	H	Time increment.
16-20	xxxxx	L1	Number of rows in data table ZIFZY.
21-25	xxxxx	L2	Number of rows in data table CDREM.
26-30	xxxxx	L3	Number of columns in data table CDREM.
31-35	xxxxx	L4	Number of rows in data table RECD.
36-40	xxxxx	NM	Polynomial order used in Adams-Moulton method of numerical integration.
41-45	xxxxxx	NOTAPE	TAPE option. If NOTAPE is equal to 1, no data tape will be printed; otherwise, one will be printed.

Line 9 Statement no. 2. Format for reading in sphere constants, and flight length.

<u>Column</u>	<u>Format</u>	<u>Variable</u>	<u>Description</u>
1-10	xxxxxx.xxx	SM	Sphere mass in kg.
11-20	xxxxxx.xxx	D	Sphere diameter in meters.
21-30	xxxx.xxxxx	GS	Magnitude of gravity at mean sea level.
31-40	xxx.xxxxxx	QLAT	Geocentric latitude of sphere.
41-50	xxx.xxxxxx	PB	Initial pressure in Newtons/m ² .
51-60	xxxxxxxxx.x	ZINT	The altitude interval at which data is desired.
61-70	xxxxxxxxx.x	ZOI	Minimum altitude allowed for the flight.
71-80	xxxxxxxxx.x	TO	Maximum time allowed for the flight.

Line 10, Statement no. 3. This statement specifies the format used for inputting the initial sphere conditions.

<u>Column</u>	<u>Format</u>	<u>Variable</u>	<u>Description</u>
1-10	xxxxxxxx.x	Y(1)	z, Altitude of sphere with respect to reference frame.
11-20	xxxxxxxx.x	Y(2)	x, Easterly displacement of sphere.
21-30	xxxxxxxx.x	Y(3)	y, Northerly displacement of sphere.
31-40	xxxxxxxx.x	Y(4)	\dot{z} , Vertical component of velocity.
41-50	xxxxxxxx.x	Y(5)	\dot{x} , Velocity in x-direction (Easterly).
51-60	xxxxxxxx.x	Y(6)	\dot{y} , Velocity in y-direction (Northerly).

- Line 11 Statement no. 4. Format used for reading of altitude z and thermal temperature T_m data. This format is only a dummy format in that the input data should include the decimal point to over-ride the decimal point specified in the format statement. The data should be ordered such that all z values are read in first in increasing order and second, the values T_m are ordered to correspond with z.
- Line 12 Statement No. 5. This statement is format used for reading all values of the drag table which is a function of both Mach and Reynolds numbers. The Reynolds numbers and Mach numbers are considered as part of the drag table and should therefore be included with drag coefficients. The table is read in columnwise. It is also necessary that the dimension statement correspond exactly with data table size.
- Line 13 Statement no. 6. Format used for reading in drag table which is a function of Reynolds number only. The format is again a dummy format since both Reynolds numbers and drag coefficients are read using the same format. The only requirement is that each card include 12 fields of 6, inclusive of decimal point.
- Lines 14-18 Statements 7-10. Formats used for listing output data.
- Lines 19-25 Statements 11-13. Formats used for printing data headings.
- Line 26 Statement no. 14. Format for writing time and sphere position data on tape.

- Line 27-29 Statements 14-15. Formats for writing flight data on radar tape. (This record is listed behind radar data with an END FILE mark between records.)
- Line 30 Read virtual mass coefficient, buoyancy force coefficient, time increment, size of arrays, polynomial order used in integration subroutine, and tape option.
- Line 31 Read-in sphere mass, diameter, geocentric latitude position, initial pressure, desired altitude interval at which a data listing is desired, minimum altitude and maximum time allowed for the flight.
- Line 32 Read initial sphere position and velocity components.
- Line 33 Read columns 1 and 2 of data table ZTZXY.
- Line 34 Read drag coefficients which are a function of Mach and Reynolds numbers.
- Line 35 Read drag coefficients which are only a function of Reynolds numbers.
- Line 36 Rewind tape unit B,3.
- Line 37 Print descriptive flight parameters.
- Line 38 Call WIND subroutine for completion of data table ZTZXY.
- Line 39 Call INITIL subroutine which sets initial conditions and calculates constants which are not varied during sphere flight.

- Line 40 Call CDEQS subroutine which evaluates equations corresponding to initial conditions for flight.
- Line 41 Print heading for 1st 12 variables to be listed.
- Line 42 Terminal velocity calculated.
- Line 43 1st twelve values for data variables are printed.
- Line 44-45 Important data variables are stored on scratch tape.
- Line 46 Logic statement used to determine whether or not to write a tape containing flight data.
- Line 47 Rewind tape unit B,5.
- Line 48 Trajectory position and time data is written on B,5.
- Line 49 Density perturbation is set equal to zero. (This is only for present purposes. The perturbation may be any quantity or function, depending on the user's requirements.)
- Lines 50-99 Comparison is made between the position of the sphere and the altitude Z_d at which data is desired. If the altitude level Z_d lies between the present sphere position Z_i and the Z_{i-1} position, a linear interpolation is performed to obtain data at altitude Z_d . This data is then stored and/or printed, according to user's option.
- Lines 100-101 Control is transferred to repeat the data computation cycle, or if the flight has exceeded the maximum time or minimum altitude allowed for the flight, control is transferred to write and/or print the data which has been stored on the scratch tape.

Lines 102-104 The scratch tape is rewound preparatory to writing flight data on tape and the END FILE mark is written indicating the completion of radar data record no. 1.

Line 105 The total number of data records is written on the radar tape.

Lines 106-119 Flight data is stored on the radar tape after the first file and also listed.

WIND SUBROUTINE

Introduction

This subroutine completes the data table ZTZXY by filling in the last three columns with values for wind velocity. The user may wish to use this subroutine only to read in wind data having the same fineness as T_m or he may desire to compute the wind structure data. (Note: This subroutine should also be used to print out special flight labels which will appear at the top of the data list sheet.)

Simple Wind Program

This program converts rough wind structure data to the same fineness as the data table. The number of wind levels read in and the Dimension statement must agree. The altitudes at which the rough wind structure data is specified must equal altitudes found in the fine data table ZTZXY.

Lines 1-3 Dimension statements identical with those of MAIN program.

Line 4 Dimension statement for rough wind structure data.

Lines 5-8 Common statements identical with lines 4-7 of MAIN.

Line 9 Format for read-in of rough wind structure data.

Line 10 Read rough wind structure data. First, all values of z,
Second, wind velocity in x-direction.

Lines 11-25 Linear interpolation of rough wind structure data is performed.
Fine data is stored in data table ZTZXY.

Line 26 Control transferred back to MAIN.

INITIL SUBROUTINE

Introduction

This subroutine calculates the coefficients used in the numerical integration subroutine, constants used throughout the program, and sets initial conditions in the program to their preassigned values.

Description

Lines 1-3 Dimension statements identical with those of MAIN program.

Lines 4-7 Common statements used throughout program.

Lines 8-34 Program constants.

Lines 35-36 Initial conditions.

Lines 37-49 Single-step integration coefficients.

Lines 50-95 Computation of multi-step integration coefficients.

Line 96 Control transferred back to MAIN program.

CDEQS SUBROUTINE

Introduction

CDEQS contains and evaluates the equations of motion associated with the falling sphere. Pertinent diagnostic messages are also printed from this subroutine.

Description

Lines 1-3 Dimension statements - same as Lines 1-3 of MAIN.

Lines 4-7 Common statements - equivalent to lines 4-7 of MAIN.

Lines 8-10 Formats for printing QM, RE, or z if variable exceeds input tabulated values.

Lines 11-21 Finds altitude interval in data table which corresponds to sphere altitude z.

Lines 22-28 Linear interpolation performed to obtain values of T_m , W_z , W_x , and W_y corresponding to altitude z.

Lines 29-32 Sphere velocity relative to wind calculated.

$$VEL = \sqrt{(\dot{z} - W_z)^2 + (\dot{x} - W_x)^2 + (\dot{y} - W_y)^2}$$

Line 33 Geometric altitude h calculated.

$$h = z + (x^2 + y^2)/2R$$

Line 34 Geocentric radial length calculated.

$$R_t = R + h$$

Lines 35-36 Magnitude of gravity g calculated.

$$g' = a_{g_s} (R/R+h)^2 - R\omega^2 \cos^2 L$$

Lines 37-38 Speed of sound

$$c = 20.046803 \sqrt{T_m}$$

Line 39 Coefficient of viscosity μ .

$$\mu = \frac{1.458 \times 10^{-6} (T_m)^{3/2}}{T_m + 110.4}$$

Line 40 Mach number

$$M = V/c$$

Lines 41-46 Pressure

$$P = P_B \exp \left\{ - \frac{M_w}{R^*} \int_{z_b}^z \frac{g w}{T_m w} dw \right\}$$

Line 47 Density

$$\rho = \frac{M_w P}{R^* T_m} + \Delta \rho$$

where $\Delta \rho$ is perturbation.

Line 48 Sphere mass. Including or excluding the induced or virtual mass is obtained by setting ALPHA equal to 0.5 or 0.0 respectively.

Line 49 Buoyancy quantity. BET is coefficient used for eliminating buoyancy force from equations of motion.

Line 50 Kinematic viscosity.

$$\eta = \frac{\mu}{\rho}$$

Line 51 Reynolds number

$$R_e = \frac{Vd}{\eta}$$

Lines 52-85 Coefficient of drag, C_d , calculated by linear interpolation of proper drag table.

Line 86 Wind response

$$\omega_c = \frac{\pi d^2 C_d V \rho}{8 m_1}$$

Lines 87-89 Drag acceleration components.

$$\bar{a}_d = -\omega_c (\bar{v} - \bar{W})$$

Lines 90-92 Components of sphere velocity.

Line 93 Gravity including acceleration due to buoyancy.

$$g' = g (1 - V_m \rho)$$

Lines 94-96 Components of sphere acceleration relative to reference frame.

Lines 97-101 Magnitude of sphere acceleration.

$$a = \sqrt{\ddot{z}^2 + \ddot{x}^2 + \ddot{y}^2}$$

Lines 102-107 Error diagnostic print statements.

Line 108 Control transferred back to calling program.

RKG SUBROUTINE

Introduction

This subroutine will solve n- differential equations by first using Runge-Kutta-Gill integration for NM data points. Control is then transferred to the multistep portion which uses the Adams-Moulton integration technique.

Description

Lines 1-3 Dimension statements equivalent to lines 1-3 of MAIN.

Lines 4-7 Common statements.

Lines 8-12 Control statements which direct control to either single or multistep integration technique.

Lines 13-20 Single step integration section which uses Runge-Kutta-Gill method.⁷

Lines 21-47 Multistep integration section which uses Adams-Moulton method.⁶

Line 48 Control transferred back to Calling Program.

CHAPTER V

EXAMPLE

INTRODUCTION

To demonstrate the use of the sphere trajectory generator program, a study of the sphere's capability of responding to wind structure of a fine nature was undertaken.

FLIGHT CONDITIONS

The parameters associated with the simulated sphere flights were selected using initial conditions typical of actual known high altitude falling sphere flights. A value for the initial pressure and the molecular temperature profile was obtained from the U.S. Standard Atmosphere, 1962.

To measure the response capability of the falling sphere, the vertical and Northerly directed wind components were set equal to zero. Because the sphere response as a function of wind layer thickness was sought, a sinusoidal function of altitude was used to produce the x-component of wind velocity, W_x . These conditions expressed in terms of their fortran expressions are:

$$ZTZXY(I, 3) = 0.$$

$$ZTZXY(I, 4) = 0. \qquad 5-1$$

$$ZTZXY(I, 5) = A_m \sin(\Omega z + \phi)$$

for $1 \leq I \leq 210$ and $\Omega = 2\pi/\lambda$.

Here λ is the wind layer thickness. The phase displacement ϕ was such that at an altitude of 30 km, W_x was equal to zero.

The main program was changed such that only values for time, x-component of sphere velocity, and the horizontal wind component W_x were printed out as a function of altitude. It was also desirable to modify the CDEQS subroutine to include the computation of W_x . This provided an improvement in the sinusoidal wave for evaluating the equations of motion over what would have been provided by interpolated values from the ZTZXY array.

Reduced meteorological data from actual flights indicate wind layer thicknesses of one-half to six kilometers are typical of fine structure at the higher altitudes. For this reason, λ values of 1/2, 1, 1.5, 2, 3, 4, and 6 kilometers were used for succeeding flights. The sphere mass and diameter was maintained respectively at 115 grams, and 1 meter for each flight.

RESPONSE CHARACTERISTICS

To illustrate the response characteristics, the data obtained using a layer thickness of 1500 meters and an amplitude of 5 meters/second is plotted in Figure 2. From the response curve several characteristics are predominant. These are: (1) the sphere responds very little to the horizontal wind at the higher altitudes, (2) there is an altitude lag between the wind and horizontal sphere velocity and (3) the horizontal velocity is displaced in the Easterly direction.

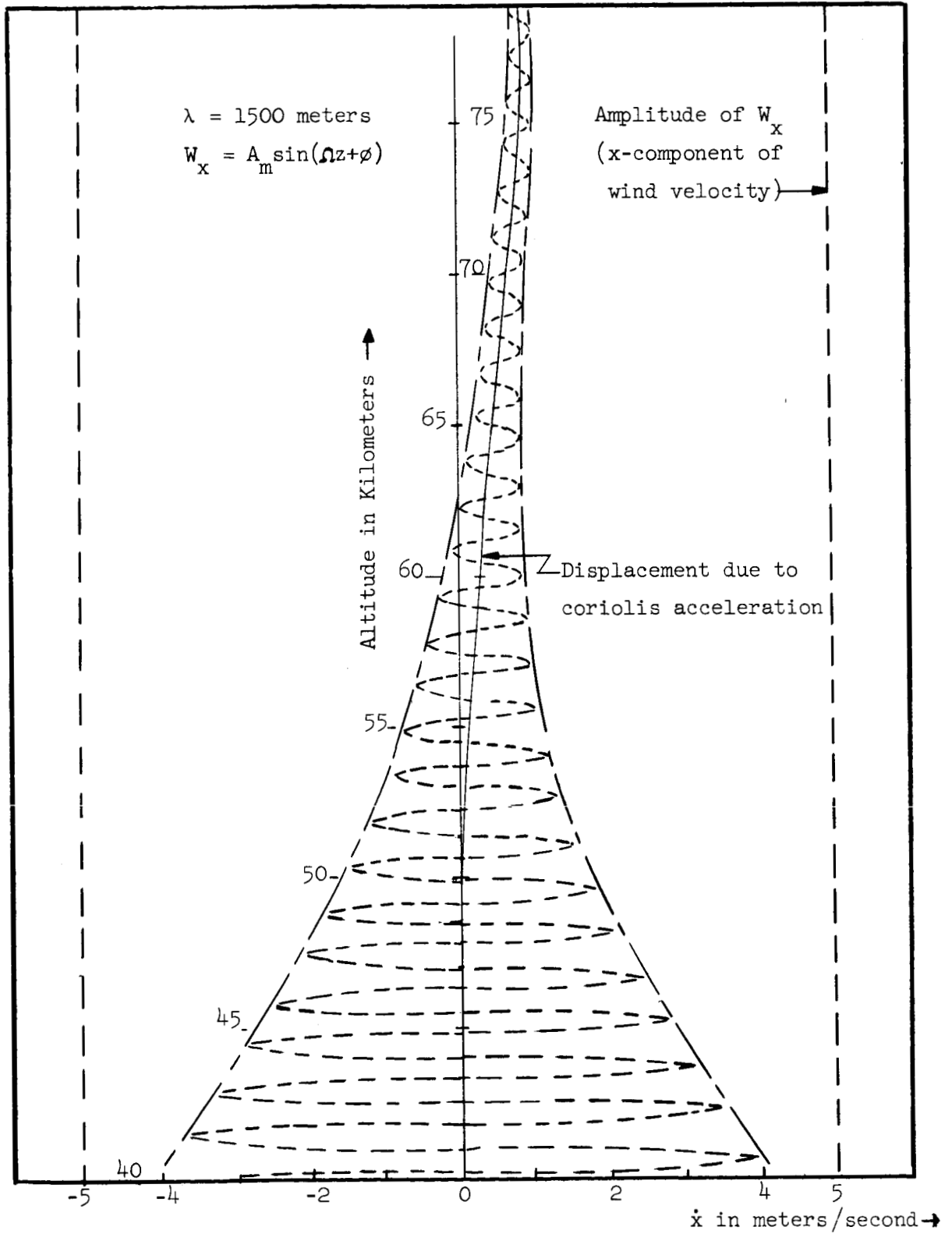


Figure 2.

Wind Response of Falling Sphere

Consider \ddot{x} from the equations of motion.

$$\ddot{x} = -\omega_c(\dot{x} - W_x) - 2\omega_z \dot{z} \cos L + 2\omega_y \dot{y} \sin L - x \left(g' / (R+h) - w^2 \right) \quad 5-2$$

The latter two terms are small and can be neglected. At the higher altitudes, i.e. above 80 km, the coriolis acceleration—the second term—is greater than the drag component, causing \ddot{x} to be positive. Therefore, the displacement of \dot{x} increases until the drag acceleration exceeds the coriolis term, after which the displacement of \dot{x} slowly approaches zero. The slow decrease in \dot{x} is indicative of the insensitivity of the sphere in responding to the horizontal winds.

Altitude Lag

The altitude lag between the horizontal wind and the x-component of sphere velocity is plotted in Figure 3.

Here it is seen that the lag is non-linear and increases with altitude. At the higher altitudes, the data became scattered. This is caused predominately by the coarseness of the data values. A time increment of 0.25 seconds was used for the computer runs. This time increment does not provide enough fine data at the higher altitudes to accurately determine the peaks of the amplitude response.

Sensitivity

The sensitivity of the sphere in responding to the horizontal wind is defined as

$$\text{Sensitivity } \sigma = \frac{\dot{x}(W_x, z)_{\max}}{A_m} \quad 5-3$$

Where A_m = amplitude of W_x .

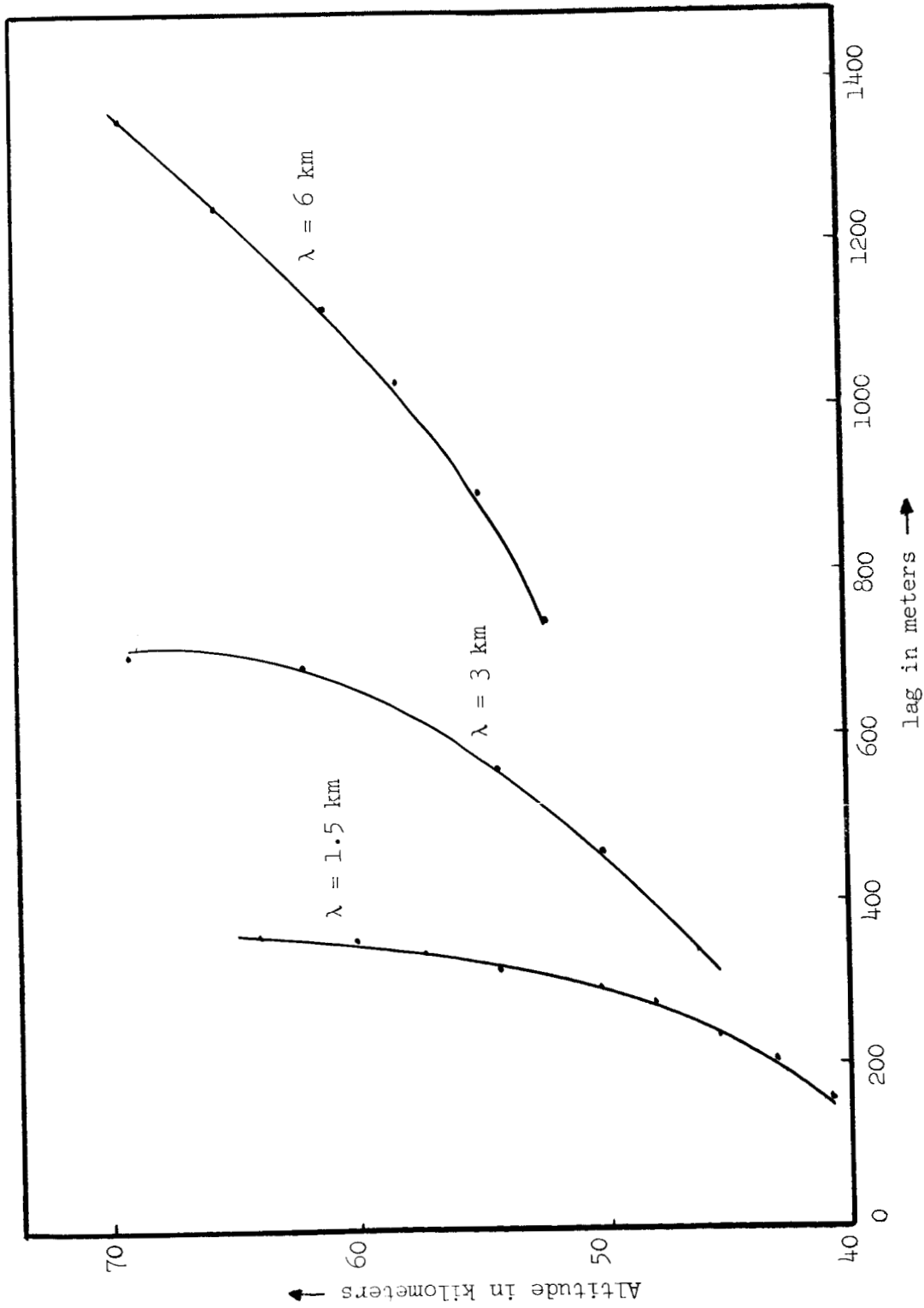


Figure 3. Altitude lag between sphere velocity \dot{x} and wind W_x .

Because of the large phase lag between \dot{x} and W_x , the sensitivity is taken as the ratio of the maximum value of \dot{x} attained in one wavelength λ to the amplitude of the sinusoidal wind A_m .

Figure 4 shows sensitivity plotted as a function of altitude and layer thickness. Superimposed also on this plot is a least square linear fit of actual rocket - meteorological data. This linear curve was reported by W. L. Webb at the Proceedings of the Fifth International Space Science Symposium, Florence, Italy, May 8-20, 1964. The intersection of Webb's curve with the computed sensitivity curves indicates the attenuation of the sphere motion associated with the respective deduced wind magnitudes used in his study.

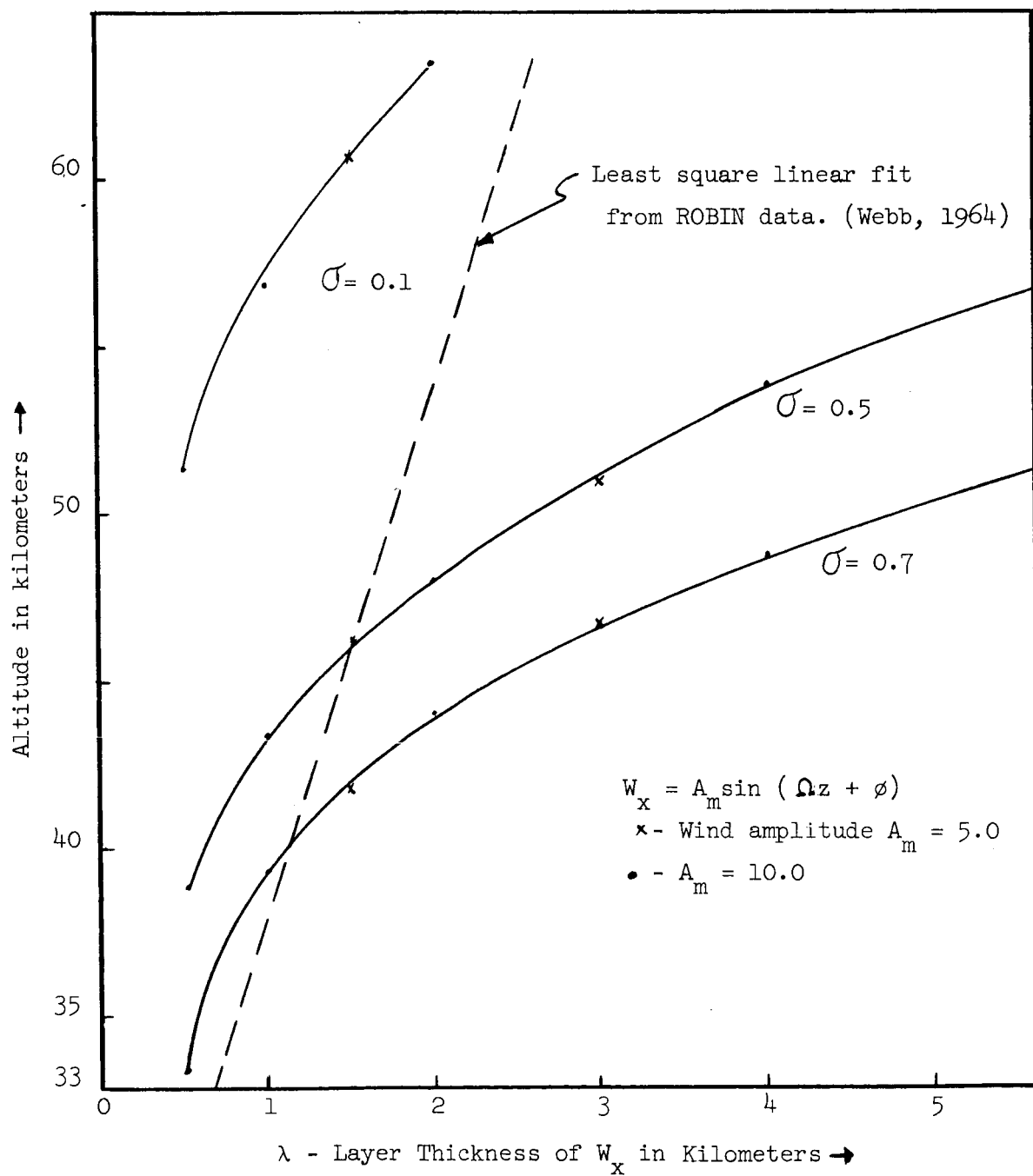


Figure 4. Sensitivity of Sphere to Horizontal Winds, W_x .

CHAPTER VI

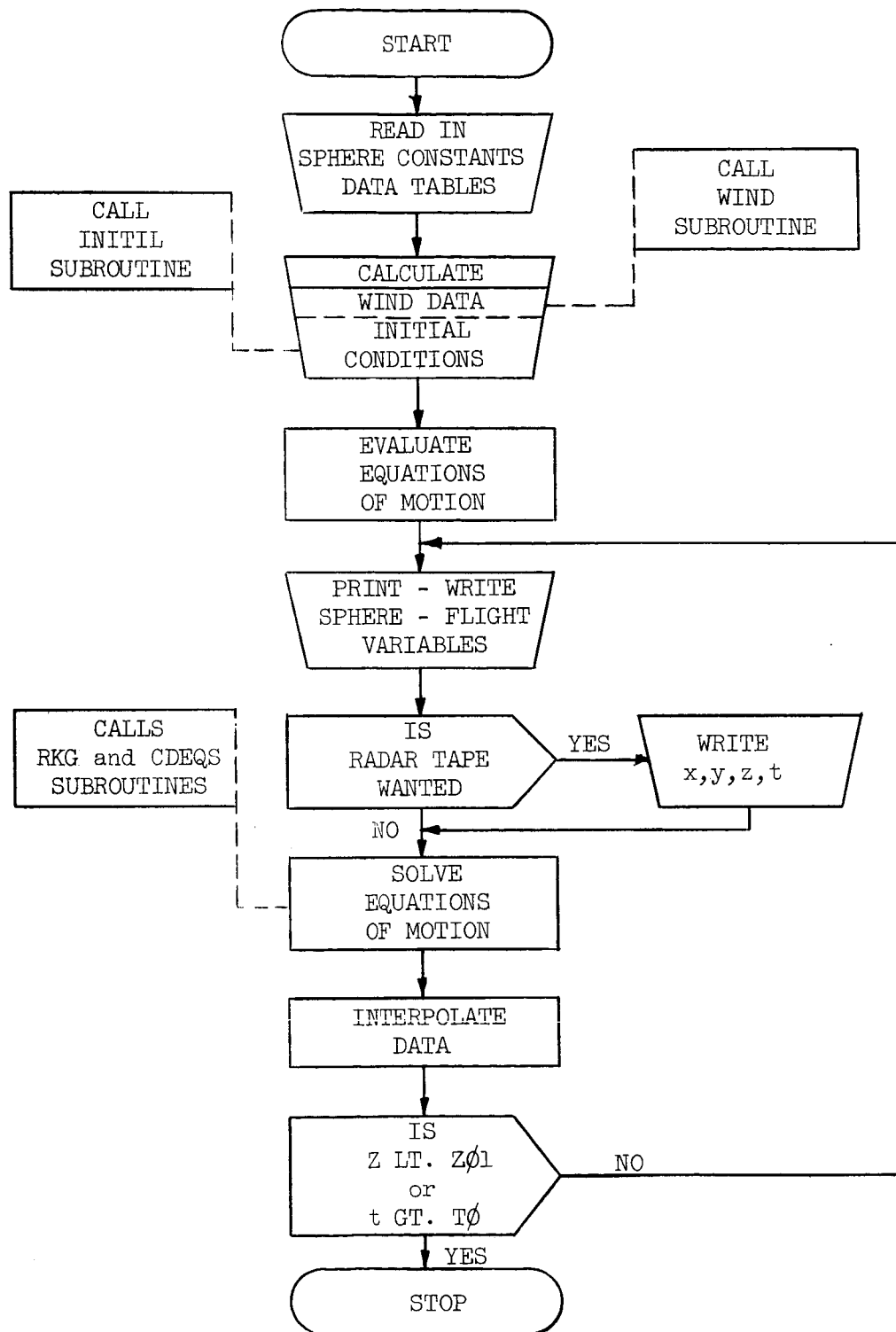
CONCLUSIONS

The sphere simulation program can be an extremely helpful tool. It can supply information desirable for preliminary design and also aid in reducing data obtained from sphere flights.

The test study of the last chapter demonstrated one of many ways in which the simulator can be used. The findings of this study using the simulator suggest the following areas for future study: (1) sphere design specifications, (2) sphere capability as a sensing device, and (3) sphere response characteristics due to complex wind structures.

The simulator program can also be applied to the problem of falling sphere data reduction. In this area, strange data phenomena can be studied, smoothing techniques designed, and complete data reduction schemes developed surrounding the program used for the present simulator program.

APPENDIX - A
FLOW DIAGRAM
with
PROGRAM LISTING



MAIN Trajectory Generator Program.

FLOW DIAGRAM OF MAIN PROGRAM

```

$13FTC MAIN
1 DIMENSION TZXZY(210,5),CDREM(22,18),RECD(24,2),Y(6),FT(27),V(6),
2 IDER(6),A(14),B(4),C(6),BETA(2,8),FNC(6,8),FI(27),GAMMA(2,8),
3 ZSUM(6),Y1(6)
4 CDPYON ' ',TI,MM,H,LAI, ZI,ZXY,CDREM,RECD,Y,PB,ALPHA,C,SM,BET,QLAT,
5 L1,L2,L3,L4,FT,ZINT,KCLD,V,DER,VEL,AC,ZO,ZD2,XD2,YD2,ROE,T,QM,RE,
6 ZD,K5,KO,NO,QL,VCL,K1,JT,IT,CCL,C1,C2,C3,C4,A,B,C,Q,BETA,FNC,IP,OC
7 3,ALPHA2,RADA,R,RL,C32,DELRCCE,CM,C5,C5
8 1 FORMAT(3F5.2,6I5)
9 2 FORMAT(2F10.3,F10.5,2F10.6,3F10.1)
10 3 FORMAT(6F10.1)
11 4 FORMAT(11OF8.3)
12 5 FORMAT(11F7.3)
13 6 FORMAT(11F6.3)
14 7 FORMAT(11F10.1)
15 8 FORMAT(F10.1,6F20.10)
16 9 FORMAT(F10.1,1PE20.8,OR2F10.3,F10.1,F10.4,1PE20.8,OP2F15.7)
17 10 FORMAT(15H PB=F10.7, 5H D= F5.1, 4H M= F10.7, 5H LAT= F10.7,
18 1 3H -F= F5.2, 7H ALPHA= F5.1, 6H BET =F5.1, 5H NH= 15)
19 11 FORMAT(11ZOH YD T WZ Z ZOD WX X XOD V ZO A )
20 1 XOD
21 2 FORMAT(11Z5H Z ZDZ ZOD XOD VT T QM C )
22 1 YOD
23 22 FORMAT(11L8H Z PB ROE VT T QM C )
24 1 RE
25 14 FORMAT(F8.1,3F10.1)
26 15 FORMAT(113F10.1,76F20.10/F10.1,1PE20.8,OP2F10.3,F10.1,F10.4,1PE20.8,
27 1OP2F15.7)
28 16 FORMAT(11I10)
29 READ 1,ALPHA,BET,H,L1,L2,L3,L4,NW,NCTAPE
30 READ 2,SM,D,G5,QLAT,PB,ZINT,ZO1,TO
31 READ 3,Y
32 READ 4,((ZTZXZY(I,J),I=1,11),J=1,2)
33 READ 5,CDREM
34 READ 6, RECD
35 REMIND 0
36 DELROE=0.
37 PRINT 10,PB,0,SM,QLAT,H,ALPHA,BET ,NH
38 CALL WIND
39 CALL INI TIL
40 CALL CDEQS
41 PRINT 11
42 V5=V(6)/OC
43 PRINT 7, TI, Y, (V(I),J=3,5), VEL,AC
44 WRITE(6) TI,Y,(V(I),J=3,5) VEL,AC,
45 1YD2,ROE,T,QM,RE,CD,PB,V5,V(6)
46 IF(NOTAPE.EQ.1) GO TO 20
47 REMIND 4
48 WRITE(4,14) TI,Y(1),Y(2),Y(3)
49 CALL RKS
50 IF(NOTAPE.EQ.1) GO TO 19
51 WRITE(4,14) TI,Y(1),Y(2),Y(3)
52 19 IF(INOLD.EQ.1) GO TO 35
53 F(1)=TI
54 DD 21J=1,6
55 IF(J.GT.3) GO TO 21
56
57 F(J+7)=V(I,J+2)
58 F(J+13)=DER(J+3)
59 21 F(J+1)Y(J)
60 F(11)=VEL
61 F(12)=AC
62 F(13)=DELROE
63 F(17)=ZD2
64 F(18)=XO2
65 F(19)=YD2
66 F(20)=ROE
67 F(21)=T
68 F(22)=OM
69 F(23)=RE
70 F(24)=CJ
71 F(25)=PB
72 F(26)=V(6)/OC
73 F(27)=V(6)
74 L21=F(2)/ZINT
75 A21=L21
76 GO TO (22,23,24),K5
77 22 F2=F(2)
78 K5=2
79 GO TO 32
80 23 K5=3
81 GO TO 25
82 24 IF(FT(2).LT.F2.AND.FT(2).LT.F(2)) GC TO 30
83 IF(FT(2).GT.F2.AND.FT(2).GT.F(2)) GC TO 30
84 25 IF(A21/A22-1.)26,33,27
85 26 X1T=(A22-ZINT-F(2))/(FT(2)-F(2))
86 G3 TO 28
87 27 X1T=(A21-ZINT-F(2))/(FT(2)-F(2))
88 28 F2=FT(2)
89 DD29=1,27
90 29 FT(J)=X1T*(FT(IJ)-F(J))+F(J)
91 GO TO 31
92 30 F2=FT(2)
93 31 PRINT7,(FT(J),J=1,12)
94 WRITE(6),(FT(J),J=1,27)
95 IP=IP+1
96 L22=L21
97 A22=A21
98 DD33=1,27
99 33 DD33=1,27
100 34 FT(J)=F(IJ)
101 IF(FT(2).LT.ZO1) GO TO 35
102 IF(TI-TO)20,20,35
103 REMIND 0
104 IF(NOTAPE.EQ.1) GC TO 41
105 END FILE 4
106 WRITE(4,16)IP
107 DD36=1,IP
108 READ(6) (FT(J),J=1,27)
109 IF(NOTAPE.EQ.1) GO TO 36
110 WRITE(4,15) (FT(J),J=1,27)
111 36 PRINT 8,FT(2),(FT(J),J=14,19)
112 IF(NOTAPE.EQ.1) GO TO 42
113 END FILE 4
114 REMIND 4
115 42 REMIND 0

```

```

116 PRINT 13
117 DJJ7I=1,IP
118 READIC(I,T(J),J=1,27)
119 37 PRINT 9,FI(12),FI(13),J=20,27)
40 STOP
END

SUBROUTINE WIND
1 DIMENSION ZTZX(Y(210,5),CDREM(22,18),RECD(24,2),Y(6),FT(27),V(6),
2 IDER(6),A(4),B(4),C(4),C(6),BETA(2,8),FNC(6,8),F(27),GAMMA(2,8),
3 ZSUM(6),YI(6)
4 COMMON V,II,NM,H,LAI, ZTZX,CDREM,RECC,Y,PB,ALPHA,D,SM,BET,QLAT,
5 LL1,L2,L3,L4,FT,ZINT,KCLD,V,DER,VEL,AC,ZO,ZD2,XD2,YC2,ROE,T,CM,RE,
6 ZCD,K5,KO,NO,Q1,VOL,K1,JT,IT,CCI,C1,C2,C3,C4,A,B,C,G,BETA,FNC,IP,OC
7 3,ALPHA2,RADA,R,RL,C32,DELRCCE,OM,OS,GS
8 N=6
9 IP=0
10 TI=0.
11 KI=1
12 K5=1
13 IT=2
14 JT=2
15 NO=1
16 KO=1
17 VOL=0.5235988*(D**3)
18 QMO=28.9644
19 RSTAR=8.31432
20 Q1=OMC/RSTAR*.001
21 OC1=0.3926991*D**0
22 OMEGA=7.292115E-05
23 OI=2.*OMEGA*COS(QLAT)
24 OZ=2.*OMEGA*SIN(QLAT)
25 OS=OI**2/4.
26 OJ=OI**01/4.
27 O5=OZ**02/4.
28 OM=OMEGA*OMEGA
29 ALPHA2=1./298.32
30 RADA=6378178.
31 R=RADA*(1.-ALPHA2*(1.+1.5*ALPHA2)**05/CM)
32 GS=GS*R*O4
33 RI=-5/R
34 OJ2=2.*O4
35 DD1J=1,N
36 I Q(I,J)=0.
37 S=0.5**0.5
38 A(1)=.5
39 A(2)=1.0-S
40 A(3)=1.0+S
41 A(4)=1.0/6.0
42 B(1)=1.0
43 B(2)=S-1.0
44 B(3)=-S-1.0
45 B(4)=-1.0/3.0
46 C(1)=0.5
47 C(2)=1.0+S
48 C(3)=1.0-S
49 C(4)=-0.5
50 LAI=1
51 CO=1.
52 KJ=1
53 2 GAMMA(KJ,I)=1.
54 K=1
55 3 GAM=0.

SUBROUTINE INITIL
1 DIMENSION ZTZX(Y(210,5),CDREM(22,18),RECD(24,2),Y(6),FT(27),V(6),
2 IDER(6),A(4),B(4),C(4),C(6),BETA(2,8),FNC(6,8),F(27),GAMMA(2,8),
3 ZSUM(6),YI(6)
4 COMMON V,II,NM,H,LAI, ZTZX,CDREM,RECC,Y,PB,ALPHA,D,SM,BET,QLAT,
5 LL1,L2,L3,L4,FT,ZINT,KCLD,V,DER,VEL,AC,ZO,ZD2,XD2,YC2,ROE,T,CM,RE,
6 ZCD,K5,KO,NO,Q1,VOL,K1,JT,IT,CCI,C1,C2,C3,C4,A,B,C,G,BETA,FNC,IP,OC
7 3,ALPHA2,RADA,R,RL,C32,DELRCCE,OM,OS,GS
8 N=6
9 IP=0
10 TI=0.
11 KI=1
12 K5=1
13 IT=2
14 JT=2
15 NO=1
16 KO=1
17 VOL=0.5235988*(D**3)
18 QMO=28.9644
19 RSTAR=8.31432
20 Q1=OMC/RSTAR*.001
21 OC1=0.3926991*D**0
22 OMEGA=7.292115E-05
23 OI=2.*OMEGA*COS(QLAT)
24 OZ=2.*OMEGA*SIN(QLAT)
25 OS=OI**2/4.
26 OJ=OI**01/4.
27 O5=OZ**02/4.
28 OM=OMEGA*OMEGA
29 ALPHA2=1./298.32
30 RADA=6378178.
31 R=RADA*(1.-ALPHA2*(1.+1.5*ALPHA2)**05/CM)
32 GS=GS*R*O4
33 RI=-5/R
34 OJ2=2.*O4
35 DD1J=1,N
36 I Q(I,J)=0.
37 S=0.5**0.5
38 A(1)=.5
39 A(2)=1.0-S
40 A(3)=1.0+S
41 A(4)=1.0/6.0
42 B(1)=1.0
43 B(2)=S-1.0
44 B(3)=-S-1.0
45 B(4)=-1.0/3.0
46 C(1)=0.5
47 C(2)=1.0+S
48 C(3)=1.0-S
49 C(4)=-0.5
50 LAI=1
51 CO=1.
52 KJ=1
53 2 GAMMA(KJ,I)=1.
54 K=1
55 3 GAM=0.

```

\$13FTC CDEQS

```

56 DD4 J=1,K
57 CJK=K+J
58 GAM=GAM+GAMMA(K,J)/(CCN*1.)
59 K=K+1
60 GAMMA(K,K)=CO-GAM
61 IF(K.LT.NM) GO TO 3
62 K=1
63 DD1111=1,NM
64 SUMT=0.
65 A4=1.
66 ILL=11-1
67 A3=ILL
68 IF(111.EQ.1) GO TO 7
69 DJ 6J=1,ILL
70 A4=A4+A3
71 A3=A3-1.
72 RDEFAC=A4
73 IF(111.EQ.1) A3=1.
74 A5=RDEFAC
75 A3=ILL
76 AJ=1.
77 DJ 9J=11,NM
78 SUMT=SUMT+GAMMA(K,J)*A5/RDEFAC
79 IF(111.EQ.1) GO TO 9
80 A5=1.
81 A3=A3+AJ
82 A5=A5*B3
83 B3=B3-1.
84 IF(B3.GT.AJ) GO TO 8
85 AJ=AJ+1.
86 9 CONTINUE
87 K=K+1
88 IF(K.EQ.3) GO TO 10
89 GO TO 11
90 SUMT=-SUMT
91 K=1
92 11 BETA(K,J,11)=SUMT
93 CJ=0.
94 KJ=KJ+1
95 IF(KJ.EQ.2) GO TO 2
96 RETURN
SUBROUTINE CDEQS
DIMENSION ZTZXV(210,5),CDREM(22,18),RECD(24,2),Y(6),ET(27),V(6),
LDER(6),A(4),B(4),C(4),Q(6),BETA(2,8),FNC(6,8),F1(27),GAMMA(2,8),
ZSUM(6),V1(6)
CJHNM N,TI,NM,H,LAI, ZTZXV,CDREM,RECC,Y,PB,ALPHA,D,SM,BET,QLAT,
LL1+L2+L3+L4+L5+L6+L7+L8+L9+L10+L11+L12+L13+L14+L15+L16+L17+L18+L19+L20+L21+L22+L23+L24+L25+L26+L27+L28+L29+L30+L31+L32+L33+L34+L35+L36+L37+L38+L39+L40+L41+L42+L43+L44+L45+L46+L47+L48+L49+L50+L51+L52+L53+L54+L55+L56+L57+L58+L59+L60+L61+L62+L63+L64+L65+L66+L67+L68+L69+L70+L71+L72+L73+L74+L75+L76+L77+L78+L79+L80+L81+L82+L83+L84+L85+L86+L87+L88+L89+L90+L91+L92+L93+L94+L95+L96
3,ALPHA2,RADA,RARI,C52,DELRCO,OM,C5,CS
1 FDRMAT(5H QM= F10.5)
2 FDRMAT(5H RE= F20.10)
3 FDRMAT(5H Z= F10.1)
Z0=V(1)
GO TO 12
11 KO=KO-1
12 IF(KO.LE.1) GO TO 37
13 IF(Z0.LE.-ZTZXV(KO,1))GC TC 11
14 IF(Z0.GE.-ZTZXV(KO,1)).AND.Z0.LE.-ZTZXV(KO+1,1)GO TO 14
15 DD 13 I=KO,LL
16 IF(ZTZXV(I,1).GT.Z0) GC TC 15
13 CONTINUE
GO TO 37
14 I=KO+1
15 DD 16J=1,5
16 ZU=ZTZXV(I,J)
17 ZL=ZTZXV(I-1,J)
18 IF(J.NE.1)GO TO 16
19 X=(Z0-ZL)/(ZU-ZL)
20 V(I,J) = X*(ZU-ZL) + ZL
21 KO=I-1
22 ZT=0.
23 DD 17J=4,6
24 ZT=ZT+(V(J)-V(I-1))*2
25 VEL=SQRT(ZT)
26 HT=V(1)+(V(2)+Y(3)+Y(31))*RI
27 RT=R+HT
28 RTZ=R+V(1)
29 V(6)=G5*(1./(1.+HT/R))*2)-C4*RTZ
30 T=V(2)
31 C5=20.0+6803*SQRT(T)
32 QNU=11.458E-06*(T+1.5)/(T+110.4)
33 QM=VEL/CS
34 IF(ND.EQ.1) GO TO 18
35 DELTAP=.5*(V(1)-Z8)*(V(6)/V(2)+GDTB)
36 P5=PB*EXP(-Q1*DELTAP)
37 Z8=V(1)
38 GD TB= V(6)/V(2)
39 ND=Z
40 RDE=Q1*PB/T +DELRCO
41 QMASSI=SM+ALPHA*RDE*VOL
42 VM=BET + VOL/QMASSI
43 QNU=QM/RDE
44 RE=VEL*QNU
45 IF(QM.LE.2.5) GO TO 24
46 IF(QM.GT.2.5.AND.RE.GT.50.) GO TO 20
47 CD=2.5-.023267*RE+.00015734*RE*RE
48 GO TO 33

```

```

56 19 KI=KI-1
57 20 IF(RECD(KI,1).GT.RE) GC TC 19
58 21 DO 21 J=KI,1,4
59 22 IF(RECD(J,1).GT.RE) GC TC 22
60 23 CONTINUE
61 24 CD= ((X-RECD(J-1,1))/(RUC(J,1))-RECD(J-1,1))*(RECD(J,2)-
62 1 RECD(J-1,2)) +RECD(J-1,2)
63 25 GC TC 33
64 26 JT=JT-1
65 27 IF(JT.LE.1) GO TO 35
66 28 IF(QM.LT.CDREM(1,J)) GC TC 23
67 29 IF(QM.GE.CDREM(1,J)).AND.(P.LE.CDREP(1,JT+1))GO TO 26
68 30 25 J=JT,1,3
69 31 IF(CDREM(1,J).GT.QM) GC TC 28
70 32 CONTINUE
71 26 J=J+1
72 33 GO TO 28
73 27 IT=IT-1
74 34 IF(IT.LE.1) GO TO 36
75 35 IF(RE.LT.CDREM(IT,1))GC TC 27
76 36 IF(P.EG.CDREM(IT,1).AND.RE.LE.CDREM(IT+1,1))GO TO 31
77 37 DO 30 I=1,L2
78 38 IF(CDREM(I,1).GT.RE) GC TC 32
79 39 CONTINUE
80 31 I=I+1
81 40 AI=(RE-CDREM(I-1,1))/(CDREM(I,1)-CDREM(I-1,1))
82 41 A2=(QM-CDREM(I-1,1))/(CDREM(1,J)-CDREM(1,J-1))
83 42 C01=CDREM(I-1,J-1)*(CDREM(1,J)-CDREM(1,J-1))
84 43 C02=CDREM(I-1,J)*(CDREM(1,J)-CDREM(1,J-1))
85 44 C0=C01*(C02-C01)*A2
86 45 C0=OC1*CD*VEL*RCR/GMASSI
87 46 ZD2=OC*(Y(4)-V(3))
88 47 YD2=OC*(Y(5)-V(4))
89 48 YD2=OC*(Y(6)-V(5))
90 49 DER(1)=Y(4)
91 50 DER(2)=Y(5)
92 51 DER(3)=Y(6)
93 52 GPRIME=Y(6)*(1-VP*RCR)
94 53 DER(4)=ZD2*O1*Y(5)-Y(3)*C3-GPRIME
95 54 DER(5)=XD2-O1*Y(4)+C2*Y(6)-Y(2)*(GPRIME/RT-OM)
96 55 DER(6)=YD2-O2*Y(5)-C3*RTZ -Y(3)*(GPRIME/RT-O5)
97 56 ACO=0.
98 57 D03AJ=4+6
99 58 ACO=ACODER(J)**2
100 59 GO TO 39
101 60 PS=INT(1,OM)
102 61 GO TO 38
103 62 GO TO 38
104 63 PRINT,RE
105 64 GO TO 38
106 65 PRINT 3,70
107 66 KOLD=1
108 67 RETURN
109 68 END

```

SUBROUTINE RKG
DIMENSION ZTZYX(210,5),CDREM(22,18),RECD(24,2),Y(6),FT(27),V(6),
1DER(6),A(4),B(4),C(4),C(6),BETA(2,8),FNC(6,8),F(27),GAMMA(2,8),
2SUM(6),YI(6)
3COMMON N,TI,NM,H,LAI, ZTZYX,CDREM,RECD,Y,PB,ALPHA,D,SM,BET,QLAT,
4L1,L2,L3,L4,FT,ZINT,KOLD,V,DER,VEL,AC,Z3,ZD2,XD2,YD2,ROE,T,OM,RE,
5ZCD,K5,K6,N0,N01,YDL,K1,JT,IT,OC1,01,02,03,04,A,B,C,Q,BETA,FNC,IP,OC
6Z,ALPHAZ,RADA,R,K1,C02,BELRCE,OM,C5,GS
7 KBT=1
8 1 D02J=1,N
9 2 FNC(I,J,LAI)=DER(J)
10 3 IF(KBT.EQ.2) GO TO 8
11 4 IF(LAI.GE.NM) GO TO 6
12 5 D05J=1,4
13 6 D03K=1,N
14 7 E=A(J)*DER(K)+B(J)*Q(K)
15 8 Y(K)=Y(K)+H*E
16 9 Q(K)=Q(K)+3.0*E+C(J)*DER(K)
17 10 GO TO (4,5,4,5),J
18 11 TI=TI+H*0.5
19 12 CALL CODEQS
20 13 IF(LAI.LT.NM) LAI=LAI+1
21 14 IF(LAI.LE.NM) GO TO 19
22 15 KJ=1
23 16 DO 7 J=1,N
24 17 YI(J)=Y(J)
25 18 D09J=1,4
26 19 SUM(J)=0.
27 20 D010J=1,NM
28 21 JJ=NM-J+1
29 22 D0101=1,N
30 23 SUM(I)=SUM(I)+BETA(KJ,J)*FAC(I,JJ)
31 24 NM=NM-1
32 25 IF(KJ.EQ.2) GO TO 13
33 26 D012J=1,NM
34 27 D012I=1,N
35 28 FNC(I,J)=FNC(I,J+1)
36 29 DO 14 I=1,N
37 30 YI(I)=YI(I)+H*SUM(I)
38 31 IF(KJ.EQ.2) GO TO 18
39 32 TI=TI+H
40 33 KJ=2
41 34 KBT=2
42 35 CALL CODEQS
43 36 DO 17 J=1,N
44 37 YI(J)=YI(J)
45 38 GO TO 1
46 39 CALL CODEQS
47 40 RETURN
48 41 END

BIBLIOGRAPHY

1. Beer, Ferdinand P. Vector Mechanics for Engineers -- Dynamics.
New York: McGraw-Hill Book Company, Inc., 1962, pages 612-613.
2. Menzel, Donald H. Fundamental Formulas of Physics. New York:
Dover Publications, Inc., 1960, pages 228-229.
3. Heiskanen, W.A. The Earth and Its Gravity Field. New York:
McGraw-Hill Book Company, Inc., 1958, page 52.
4. "Gravity," Encyclopedia Americana. International Edition,
New York: Americana Corporation, 1965.
5. Peterson, J.W. and McWatters, K.D. "The Measurement of Upper
Air Density and Temperature by Two Radar-Tracked Falling
Spheres," Technical Report, The University of Michigan:
College of Engineering, March 1963, page 41.
6. Henrici, Peter. Discrete Variable Methods in Ordinary Differential
Equations. New York: John Wiley and Sons, Inc. 1962, pages
193-198.
7. Ralston, Anthony and Wilf, Herberts. Mathematical Methods for
Digital Computers. New York: John Wiley and Sons, Inc.,
1962, pages 110-111.
8. Webb, W.L. "Scale of Stratospheric Detail Structure," Space
Research V. Proceedings of the Fifth International Space
Science Symposium, May 8-20, 1964, Amsterdam: North-Holland
Publishing Co., 1965, pages 997-1006.
9. Peterson, J.W. "Atmospheric Measurements over Kwajalein Using
Falling Spheres," The University of Michigan: College of
Engineering, Final Technical Report, January 1965.
10. Engler, Nicholas A. "Development of Methods to Determine Winds,
Density, Pressure and Temperature From the Robin Falling
Balloon," University of Dayton Research Institute, Dayton,
Ohio, 1965.
11. Brockman, William E. "Computer Programs in Fortran and Balgol
for Determining Winds, Density, Pressure, and Temperature
From the Robin Falling Balloon," University of Dayton Research
Institute, Dayton, Ohio, January 1963.
12. Dubin, Maurice. U.S. Standard Atmosphere, 1962. Washington, D.C.,
U.S. Government Printing Office, 1962.

PART II

RADAR SIMULATOR

A brief review of the performance and specifications of the Instrumentation Radar Set AN/FPS-16 suggests the following principle features to be included in the Radar Simulator

- a) coordinate transformation to those of the radar
- b) range resolver error
- c) random (gaussian) noise on each radar coordinate
- d) digital data granularity

Bias errors and other features such as those associated with dynamic tracking properties, digital encoder and gear-train non-linearities, and propagation anomalies were not specifically characterized in the present simulator.

The coordinate transformation consists of the transformation of sphere position from the rectilinear coordinates of the trajectory generator to slant range, azimuth, and elevation angles associated with a radar site at x_p , y_p , z_p (radar parallax in meters). Slant range is the straight line distance between the radar site and sphere in yards. Azimuth is the clockwise angle from north in the x-y plane in angular mils (6400 mil/rev.). Elevation is the angular position of the sphere from the x-y plane at the radar site, expressed in angular mils. This error-free radar data are included on the output tape of the Radar Simulator for optional use.

The range resolver error is a function of slant range which is added to slant range, and which is cyclic with period 4000-yards. For generality it is specified by input at 50 equidistant points over the

4000-yard interval and is linearly interpolated. A nominal function for this error is

$$-r \cos \frac{2\pi}{2000} R$$

with

$$1.2 \leq r \leq 2 \text{ yards.}$$

It is noted, however, that preliminary measurements made in this study on radar recordings of an actual meteorological flight (Appendix A) indicate amplitudes r in excess of 5 yards.

As an approximation to the overall (higher frequency) noise contained in radar data, three random independent variables, each having approximately normal distributions with standard deviations specified in the input, are added respectively to slant range, azimuth, and elevation. Conversations with radar data analysis personnel at White Sands Missile Range indicates that the noise in FPS-16 data appear to be essentially random independent point to point even for the higher data rates of 50 points per second. Nominal values of the standard deviations are

$$\begin{aligned} \sigma_R &= 3.3 \text{ yards} \\ \sigma_A &= 0.2 \text{ mil} \\ \sigma_E &= 0.1 \text{ mil} \end{aligned}$$

The random number generator used in the radar simulator is an addition or Fibonacci type generator in which only the right-most three decimal digits are retained. The uniformly distributed variable obtained is given a normal or gaussian distribution with zero mean and unit standard deviation by

the transformation¹

$$N = \text{sgn}(r - .5) \left[v - \frac{a_0 + a_1 v + a_2 v^2}{1 + b_1 v + b_2 v^2 + b_3 v^3} \right]$$

$$v = \sqrt{-2 \log_e 0.5(1 - |1 - 2r|)}$$

$$a_0 = 2.51517 \quad a_1 = 0.802853 \quad a_2 = 0.010328$$

$$b_1 = 1.432788 \quad b_2 = 0.189269 \quad b_3 = 0.001308$$

The gaussian variable is multiplied by the appropriate standard deviation at the time it is added to the radar coordinate.

The digital data system of the FPS-16 produces slant range as 20-bit data with a granularity of 1/2 yard (524,288 yards maximum value), and azimuth and elevation as 17-bit data with granularity of 0.0488 mils (6400 mils maximum value). These properties are included in the Radar Simulator by dividing by the granular unit, truncating at the units digit, and multiplying to restore the scale as follows.

$$R = 0.5(2R)_{\text{integer}}$$

$$A = 0.0488(A/0.0488)_{\text{integer}}$$

$$E = 0.0488(E/0.0488)_{\text{integer}}$$

Where the parenthetical quantities subscripted "integer" are computed only to the units digit.

¹Juncosa, M.L., "Random Number Generation on BRL High-Speed Computing Machines", Report 855 Ballistics Research Laboratory, Aberdeen, Md.

```

0  SIBFTC MAIN
1      DIMENSION RN(3),RC(3),RRE(50),TABLE(3)
2      DO11I=1,50
3      11 RRE(I)=0.
5      READ 2,ZP,XP,YP,SIGMAR,SIGMAA,SIGMAE,RREA
6      IF(RREA.EQ.0.)READ3,RRE
11     1  FORMAT(F8.1,3F10.1)
12     2  FORMAT(3F8.1,4F5.1)
13     3  FORMAT(16F5.1)
14     REWIND 4
15     REWIND 8
16     CV=3200.0/3.1415927
17     ASSIGN 30 TO L
20     CALL EOFRET(4,L)
21     6  READ(4,1)T,Z,X,Y
22     ZR=Z-ZP
23     XR=X-XP
24     YR=Y-YP
25     Y1=XR*XR+YR*YR
26     RC(1)=(SQRT(ZR*ZR+Y1))*1.093613
27     RC(2)=(ATAN2(XR,YR))*CV
30     IF(XR.LT.0.)RC(2)=6.231853+RC(2)
33     XY=SQRT(Y1)
34     RC(3)=(ATAN2(ZR,XY))*CV
35     TABLE(1)=RC(1)
36     TABLE(2)=RC(2)
37     TABLE(3)=RC(3)
40     CALL NUMBRE(RN)
41     DRC=RC(1)-4000.*FLOAT(INT(RC(1))/4000)
42     IF(RREA.NE.0.)GO TO 14
45     IRC=DRC/80.
46     DDRC=DRC-FLOAT(IRC)*80.
47     RREF=DDRC*(RRE(IRC+1)-RRE(IRC))/80.+RRE(IRC)
50     GO TO 15
51     14 RREF=-RREA*COS (DRC*6.2831853/2000.)
52     15 CONTINUE
53     10 RC(1)=RC(1)+SIGMAR *RN(1)+RREF
54     RC(2)=RC(2)+SIGMAA*RN(2)
55     RC(3)=RC(3)+SIGMAE*RN(3)
56     L1=2.*RC(1)
57     L2=RC(2)/0.0488
60     L3=RC(3)/0.0488
61     RC(1)=FLOAT(L1)/2.
62     RC(2)=FLOAT(L2)*.0488
63     RC(3)=FLOAT(L3)*.0488
64     WRITE(8,4) T, TABLE, RC
65     4  FORMAT(F8.2,3F10.2,10X,3F10.2)
66     GO TO 6
67     30 REWIND 4
70     REWIND 8
71     STOP
72     END

```

```
0 $IBFTC NUMBRE
1     SUBROUTINE NUMBRE(RN)
2     DIMENSION RN(3)
3     IF(I.EQ.1) GO TO 4
6     R=89.
7     RR=155.
10    Z=155.
11    I=1
12    4  DO40K=1,3
13    RR=RR+R
14    R=Z
15    IF(RR-1000.)10,10,20
16    20 RR=RR-1000.
17    10 RX=RR/1000.
20    Z=RR
21    V=SQRT(-2.*ALOG(.5*(1.-ABS(1.-2.*RX))))
22    D=1.+1.432788*V+.189269*V**2+.001308*V**3
23    DN=2.515517+.802853*V+.010328**2
24    IF(RX-.5)15,15,25
25    15 RN(K)=- (V-DN/D)
26    GO TO 40
27    25 RN(K)= (V-DN/D)
30    40 CONTINUE
32    RETURN
33    END
```

APPENDIX A

RANGE RESOLVER ERROR

The range resolver error, $r(R)$, in the AN/FPS-16 radar is associated with a mechanical device which rotates 360° during each 4000 yards of slant range, and therefore is periodic in slant range.

$$r(R) = r(R-4000)$$

Typically this error exhibits two sinusoidal-like cycles per 4000-yard period, and hence appears in the data to have a period of 2000 yards. The amplitude of this periodic positional error is represented in manufacturer's reports as being about two yards (four yards peak-to-peak), or one yard with special preflight adjustment. Experience at White Sands Missile Range indicates smaller amplitudes of about 1.5 yards. These, of course, are all within the radar specifications of position accuracy.

A simple calculation, however, shows that this very small cyclic perturbation may introduce observable oscillations in the density function deduced from the radar track of the meteorological falling sphere. Suppose the cyclic perturbation in slant range is given by

$$r = -|r| \sin \omega R$$

The associated perturbation on acceleration in slant range is

$$\ddot{r} = |r| \omega (\omega \dot{R}^2 \sin \omega R - \ddot{R} \cos \omega R)$$

Assigning nominal values

$$\begin{aligned} \dot{R} &= 80 \text{ yd/sec} \\ \ddot{R} &= 0.2 \text{ yd/sec}^2 \\ \omega &= 2\pi/2000 = 0.003 \text{ yd}^{-1} \\ |r| &= 2 \text{ yd} \end{aligned}$$

which approximate those of a ROBIN sphere at mid-flight, the amplitude of the acceleration oscillation is seen to be about 0.1 yd/sec^2 . Oscillations having both amplitude and period of this magnitude are observed in ROBIN density data, and have been reported by Engler (1963).

To further establish the connection between the range resolver error and observed fluctuations in falling sphere density data, it was proposed to extract from real flight data any cyclic component in slant range having periodicity 4000 yards. This would at first appear hopeless because a) the expected perturbation amplitude is only a few times the magnitude of the granularity of the radar data, b) the frequency of the perturbation was extremely low, and c) the data sample from any given flight covers relatively few cycles of the perturbation. However, if, in fact, the supposed error source manifests itself in the density plots, then it should be amenable to extraction.

It is first noted that the range resolver error, having 4000 yard period in range, can introduce perturbations in the data with frequencies only down to $\dot{R}/4000$ cps. It was therefore attempted to eliminate from the data all frequencies lower than this. The approach was to generate an appropriate smooth function from the data and subtract this from the raw data.

The facts that (a) the small perturbations in position data may become significant in the second derivative (from which density is obtained) and (b) the real motions of the sphere are caused by relatively slow varying forces (which are proportional to acceleration), suggests that acceleration would be the appropriate quantity to smooth. A numerical scheme for generating

a smooth second derivative (Schramm and Scott 1963) was adapted to the problem. The smoothing interval was adjusted by a digital computer program so that it remained constant in the dependent variable (slant range) rather than in the dependent variable (time). In this way a smooth acceleration was obtained which exhibited a sharp cut off frequency in slant range. Integration of this smooth acceleration provided the desired smooth position, \bar{R} .

Since the nature of the cyclic perturbation within its 4000-yard period was assumed completely unknown (higher frequency components could be present) the remaining step allowed only some form of signal integration, ie, some procedure for determining the signal which was common to, or persisted in, successive 4000-yard segments of the data. The chosen method, in effect, superposed successive 4000-yard segments and computed the mean value in small sub-intervals.

Available data and funds allowed a limited processing of one flight record (ARCAS/ROBIN/FPS-16, Wallops Island flight W67-3279, 1 February, 1962, approximate apogee 190 kft). The results are shown in the accompanying table and figures.

The falling sphere trajectory in this radar record provides only about six successive 4000-yard intervals and the excursions assignable to actual sphere motions have amplitudes an order of magnitude greater than that of the cyclic perturbation. As the range rate, \dot{R} , decreases, more time is available during a range interval (4000-yards) for the sphere real accelerations to come into play and "hide" the nevertheless-present cyclic perturbation. In turn, more intervals are required in the signal integration

to discern the cyclic perturbation. Thus the cyclic perturbation cannot be evaluated accurately from the sphere data of this flight. It is expected that satisfactory results could be obtained in other flights where the range rate and data sample are large, as in high-apogee flights, and where the radar line-of-sight lies close to the sphere trajectory, or where the real motion of the sphere is relatively smooth. None of these conditions appear to exist in the given flight. It was not investigated how clearly the density function deduced from this radar record exhibits fluctuations of the type under discussion.

The desired conditions for evaluating the cyclic perturbation were found, however, in the upleg portion of the radar record, during which the rocket rather than the sphere was tracked. It is claimed that the perturbation is present throughout the radar record and having evaluated it from the upleg data, it should be subtracted from the downleg or sphere data.

Figure I is a plot of the difference function (raw range less the smoothed range) for the upleg portion of the flight. Figure II shows the result of the superposition (signal integration) of fifteen successive 4000-yard intervals excluding the first interval. Also displayed in Figure II is a typical measured range resolver error according to D. K. Barton (1964).

Several features are noted from the figures:

1. The periodicity in range and the correlation with the 4000-yard-per-revolution range resolver is clearly evident.
2. At no point does the perturbation appear to vanish. It is plausible that it is present in the entire record.

R: W67-3279, 2-1-62, AN/FPS-16
 12*36*10.0 ≤ T < 12*38*18.2 (APOGEE)

\bar{R} : UDIRSIT = MF = 15, MB = 1, RWNDΦ = 2000, RSTART = 1901.496

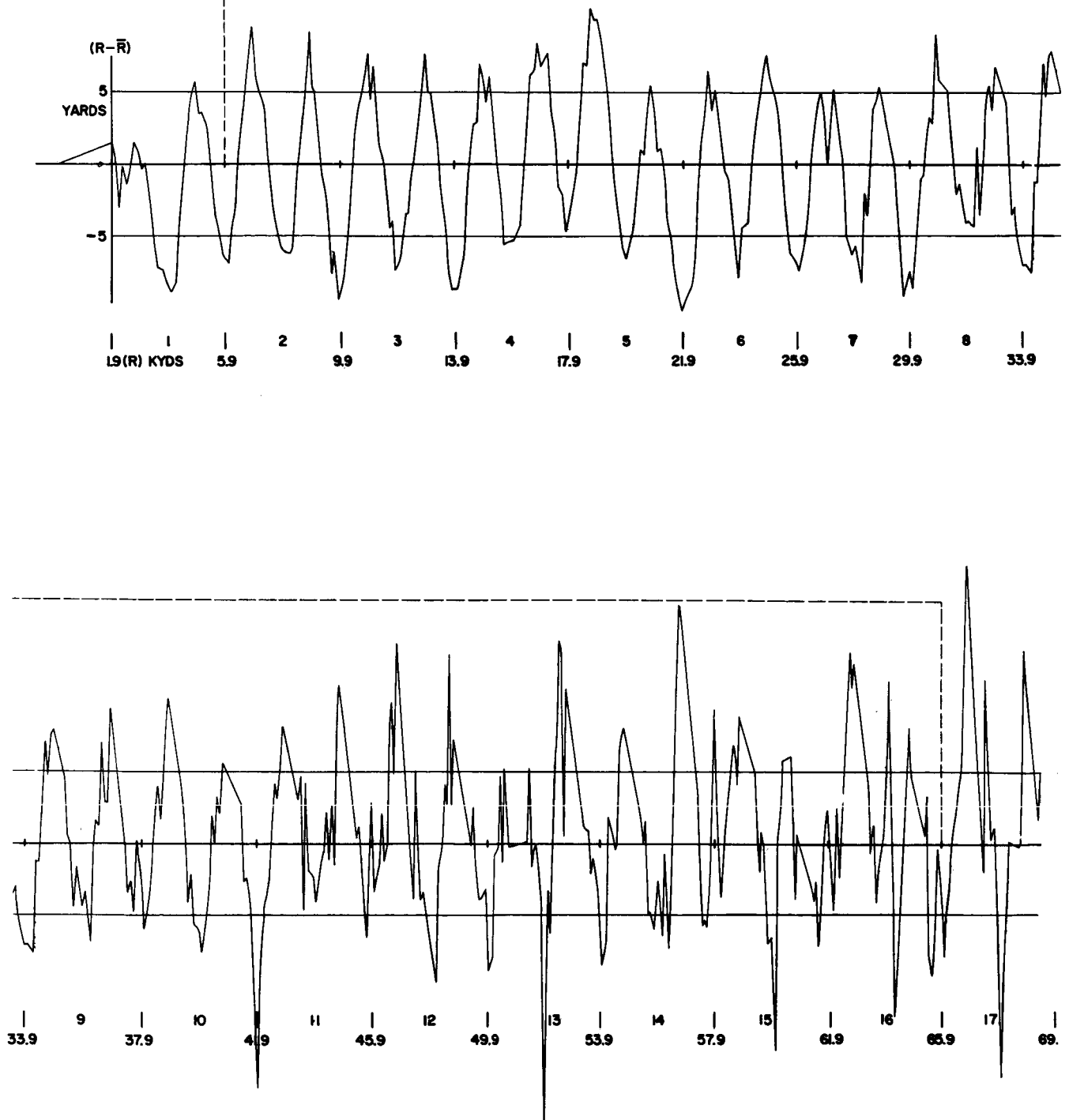


Fig. I. A Plot of the Difference Between the Raw and Smooth Range Functions.

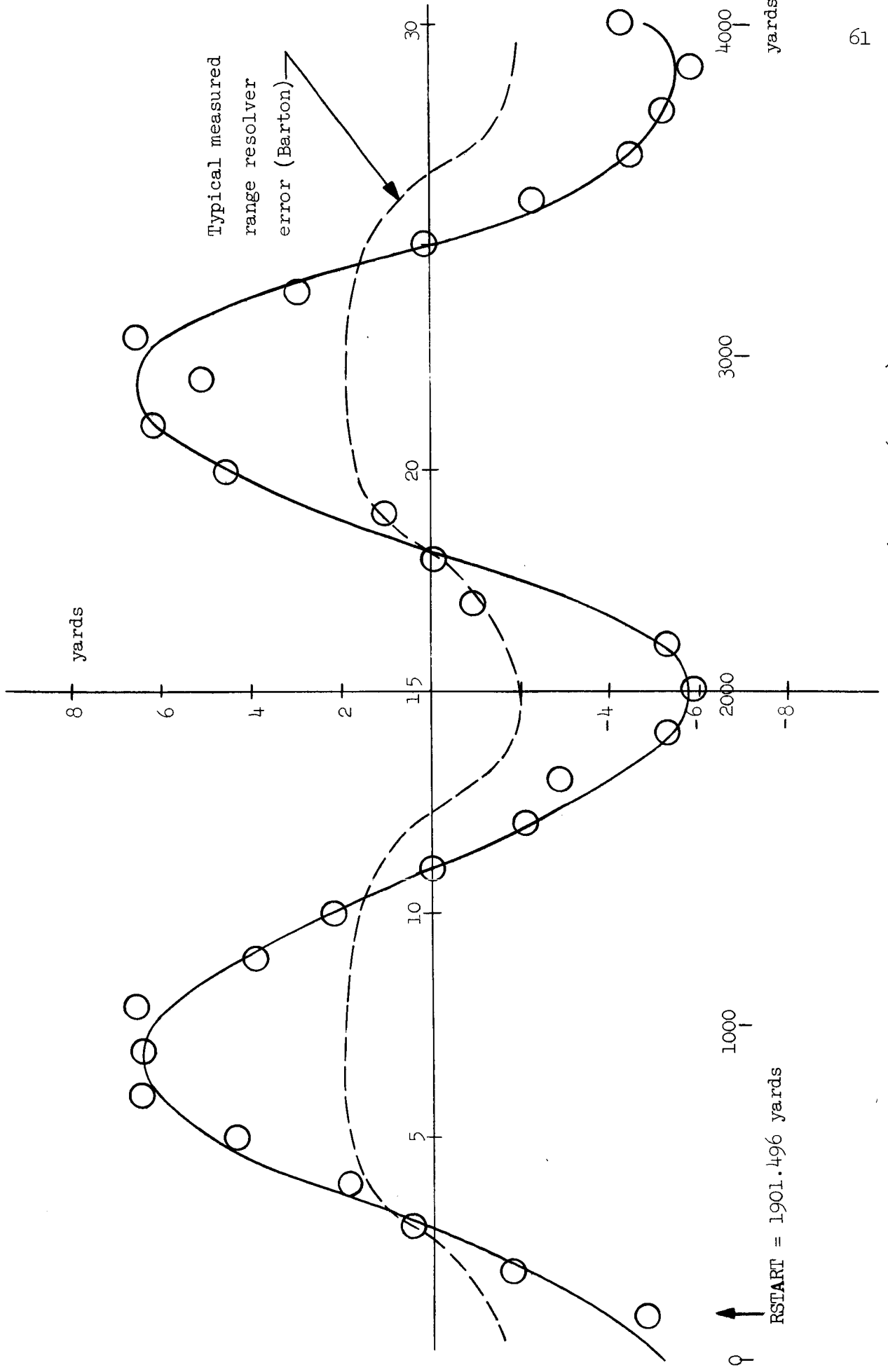


Fig. II. Cyclic Radar Range Perturbation (Flight W67-3279)

3. The amplitude of the cyclic perturbation in this data is about three times that represented as typical of measured range resolver error.
4. The initial transient of the smoothing process is confined well within the first 4000-yard interval of data. Data from this interval was not included in the signal integration process.
5. The smooth range function features very small bias. The mean value over successive 4000-yard intervals generally remained an order of magnitude smaller than the respective root-mean-square values. This indicates that the desired low frequency content was retained in \bar{R} by the smoothing process.
6. The sudden large change in acceleration due to cessation of rocket thrust (burn-out) causes the apparent discontinuity observed at the beginning of the fifth 4000-yard interval. The smoothing process allows the application of a priori knowledge of acceleration discontinuities and will enable in future improvements, if desired, the elimination of this apparent discontinuity and the associated disturbance of the mean in its neighborhood.
7. The curve beyond the tenth interval (range = 42 kyd, altitude = 34 km) begins to display increasingly erratic behavior. This perhaps is due to other radar errors. Though over twenty successive 4000-yard intervals of range data were processed and plotted, only the second through fifteenth were included in the signal integration process, arbitrarily because of the lower rms values associated with these intervals. Subsequent observation of the plotted data suggests that the result from the signal integration process would be improved

if the more erratic intervals were not included. Further study could produce appropriate computational techniques which would enable selective rejection of poor data intervals in the signal integration process.

Table I lists the root-mean-square value and mean value of the difference function for each 4000-yard interval, together with the initial value of time, smoothed range, range rate, and range acceleration in each interval.

The difference between successive values of initial smoothed range varies from 4000-yards because of the granularity in the data resulting from the sampling used in the smoothing process. In this particular case a sampling of 30 points/4000-yard interval was used, resulting in a granularity of about 133 yards per point. Furthermore, this granularity varies from point to point because the nearest raw data point was taken in preference to computing an interpolated point from the raw data. The use of "adjusted" raw data, such as obtained by averaging or by interpolating, will generally lead to failure because in general the accuracy of averaging or interpolating (or of assigning the value of the independent variable, time) will be insufficient to preserve the necessary fractional-yard precision associated with the cyclic perturbation. Further study could lead to optimization of the several parameters associated with the smoothing process and would undoubtedly improve these results. Nevertheless the objective of extracting and evaluating this error from meteorological falling sphere radar data is demonstrated, and the feasibility of eliminating this error operationally through data processing is indicated.

TABLE I

Interval (nr)	t_1 (hr:min:sec)	ΔR rms (yd)	ΔR mean (yd)	\bar{R}_1 (yd)	\dot{R}_1 (yd/sec)	\ddot{R}_1 (yd/sec ²)
1	12:36:10.0	4.50	-1.85	1,901.5	396.6	26.4
2	12:36:18.1	5.38	-0.22	6,108.1	660.8	37.1
3	12:36:23.4	4.87	-0.39	10,129.8	862.7	44.4
4	12:36:27.6	4.79	1.27	14,177.4	1,076.4	58.7
5	12:36:31.0	5.90	0.80	18,171.5	1,257.0	36.7
6	12:36:34.3	4.80	-0.03	22,215.4	1,180.7	-26.8
7	12:36:37.8	4.78	-0.97	26,205.3	1,106.8	-13.3
8	12:36:41.5	4.21	0.16	30,190.7	1,047.8	-12.8
9	12:36:45.4	4.52	0.31	34,178.6	995.9	-11.1
10	12:36:49.5	5.39	-0.42	38,176.2	954.8	- 8.5
11	12:36:53.6	4.53	0.41	41,993.1	905.2	- 9.1
12	12:36:58.3	5.82	0.56	46,152.5	863.7	- 9.0
13	12:37:03.0	6.47	0.41	50,100.9	813.4	-10.4
14	12:37:08.1	6.72	0.94	54,142.9	772.5	- 9.0
15	12:37:13.4	5.01	-0.16	58,089.8	719.2	- 7.8
16	12:37:19.1	6.54	1.35	62,045.6	670.1	- 6.2
17	12:37:25.3	7.88	0.50	66,035.8	612.4	- 7.3
18	12:37:32.1	8.81	0.04	70,021.7	559.4	- 7.2
19	12:37:39.7	11.55	-1.86	74,035.7	493.6	- 7.7
20	12:37:48.4	9.68	-0.91	78,054.4	426.8	- 6.8
21	12:37:58.6			82,060.9	344.9	-15.7

REFERENCES

- Barton, David K. Radar System Analysis. Prentice-Hall, Inc.
New Jersey, 1964, page 375.
- Schramm, Roland C. and Maceo T. Scott, "Derivative Information Recovery
by a Selective Integration Technique (DIRSIT)," Technical Memorandum
1040, White Sands Missile Range, New Mexico, November 1962.
- Engler, Nicholas A. "Method of Determining Winds, Density, Pressure,
and Temperature from the ROBIN Falling Balloon," paper presented
at Conference on Structure of the Stratosphere-Mesosphere, El Paso,
Texas, 19 November 1963.